Delft University of Technology

Adaptive Laboratory Evolution and Reverse Engineering of Single-Vitamin Prototrophies in Saccharomyces cerevisiae

Perli, Thomas; Moonen, Dewi P.I.; van den Broek, Marcel; Pronk, Jack T.; Daran, Jean Marc

Important note
To cite this publication, please use the final published version (if applicable).
Please check the document version above.

American Society for Microbiology

Applied and Environmental Microbiology®

Adaptive Laboratory Evolution and Reverse Engineering of Single-Vitamin Prototrophies in *Saccharomyces cerevisiae*

Thomas Perli,[a] Dewi P. I. Moonen,[a] Marcel van den Broek,[a] Jack T. Pronk,[a] Jean-Marc Daran[a]

aDepartment of Biotechnology, Delft University of Technology, Delft, The Netherlands

ABSTRACT Quantitative physiological studies on *Saccharomyces cerevisiae* commonly use synthetic media (SM) that contain a set of water-soluble growth factors that, based on their roles in human nutrition, are referred to as B vitamins. Previous work demonstrated that in *S. cerevisiae* CEN.PK113-7D, requirements for biotin were eliminated by laboratory evolution. In the present study, this laboratory strain was shown to exhibit suboptimal specific growth rates when either inositol, nicotinic acid, pyridoxine, pantothenic acid, *para*-aminobenzoic acid (*p*ABA), or thiamine was omitted from SM. Subsequently, this strain was evolved in parallel serial-transfer experiments for fast aerobic growth on glucose in the absence of individual B vitamins. In all evolution lines, specific growth rates reached at least 90% of the growth rate observed in SM supplemented with a complete B vitamin mixture. Fast growth was already observed after a few transfers on SM without *myo*-inositol, nicotinic acid, or *p*ABA. Reaching similar results in SM lacking thiamine, pyridoxine, or pantothenate required more than 300 generations of selective growth. The genomes of evolved single-colony isolates were resequenced, and for each B vitamin, a subset of non-synonymous mutations associated with fast vitamin-independent growth was selected. These mutations were introduced in a non-evolved reference strain using CRISPR/Cas9-based genome editing. For each B vitamin, the introduction of a small number of mutations sufficed to achieve a substantially increased specific growth rate in non-supplemented SM that represented at least 87% of the specific growth rate observed in fully supplemented complete SM.

IMPORTANCE Many strains of *Saccharomyces cerevisiae*, a popular platform organism in industrial biotechnology, carry the genetic information required for synthesis of biotin, thiamine, pyridoxine, *para*-aminobenzoic acid, pantothenic acid, nicotinic acid, and inositol. However, omission of these B vitamins typically leads to suboptimal growth. This study demonstrates that, for each individual B vitamin, it is possible to achieve fast vitamin-independent growth by adaptive laboratory evolution (ALE). Identification of mutations responsible for these fast-growing phenotypes by whole-genome sequencing and reverse engineering showed that, for each compound, a small number of mutations sufficed to achieve fast growth in its absence. These results form an important first step toward development of *S. cerevisiae* strains that exhibit fast growth on inexpensive, fully supplemented mineral media that only require complementation with a carbon source, thereby reducing costs, complexity, and contamination risks in industrial yeast fermentation processes.

KEYWORDS *Saccharomyces cerevisiae*, adaptive mutations, evolutionary engineering, media, nutritional requirements, prototrophy, reverse genetic analysis, vitamin biosynthesis

Chemically defined media for cultivation of yeasts (CDMY) are essential for fundamental and applied research. In contrast to complex media, which contain non-defined components such as yeast extract and/or peptone, defined media enable

FIG 1 Schematic representation of the *de novo* biosynthetic pathways for the B vitamins biotin (A), nicotinic acid (B), *myo*-inositol (C), pantothenate (D), *p*ABA (E), and pyridoxine and thiamine (F) in *S. cerevisiae* (5). Vitamins that are usually added to the chemical defined media for cultivation of yeasts are shown in light blue.

generation of highly reproducible data, independent variation of the concentrations of individual nutrients, and, in applied settings, design of balanced media for high-biomass-density cultivation and application of defined nutrient limitation regimes (1, 2). CDMY such as yeast nitrogen base (YNB) and Verduyn medium are widely used in research on *Saccharomyces* yeasts (2, 3). In addition to carbon, nitrogen, phosphorous, and sulfur sources and metal salts, these media contain a set of seven growth factors: biotin (B_7), nicotinic acid (B_3), inositol (B_8), pantothenic acid (B_5), *para*-aminobenzoic acid (*p*ABA) (formerly known as B_{10}), pyridoxine (B_6), and thiamine (B_1). Based on their water solubility and roles in the human diet, these compounds are all referred to as B vitamins, but their chemical structures and cellular functions are very different (4). Taking into account their roles in metabolism, they can be divided into three groups: (i) enzyme cofactors (biotin, pyridoxine, and thiamine), (ii) precursors for cofactor biosynthesis (nicotinic acid, *p*ABA, and pantothenic acid), and (iii) inositol, which is a precursor for phosphatidylinositol and glycosylphosphatidylinositol anchor proteins (5).

Previous studies demonstrated that *Saccharomyces* species are bradytroph for some B vitamins; growth does not strictly depend on addition of all of these compounds, but their omission from CDMY typically results in reduced specific growth rates (6–8). These observations imply that the term "vitamin," which implies a strict nutritional require-ment, is in many cases formally incorrect when referring to the role of these com-pounds in *Saccharomyces cerevisiae* metabolism (5). In view of its widespread use in yeast physiology, we will nevertheless use it in this paper.

The observation that *Saccharomyces* yeasts can *de novo* synthesize some or all of the "B vitamins" included in CDMY is consistent with the presence of structural genes encoding the enzymes required for their biosynthesis (Fig. 1 [5]). However, as illustrated by recent studies on biotin requirements of *S. cerevisiae* CEN.PK113-7D (5, 9), a full complement of biosynthetic genes is not necessarily sufficient for fast growth in the absence of an individual vitamin. In the absence of biotin, this strain grew extremely slowly ($\mu < 0.01$ h^{-1}), but fast biotin-independent growth was obtained through prolonged adaptive laboratory evolution (ALE) in a biotin-free CDMY. Reverse engi-neering of mutations acquired by evolved strains showed that, along with mutations in the plasma membrane transporter genes *TPO1* and *PDR12*, a massive amplification of *BIO1* was crucial for fast biotin-independent growth of evolved strains (10). These results illustrated the power of ALE in optimizing microbial strain performance without *a priori* knowledge of critical genes or proteins and in unravelling the genetic basis for

industrially relevant phenotypes by subsequent whole-genome sequencing and re-verse engineering (11, 12).

Elimination of vitamin requirements could enable cost reduction in the preparation of defined industrial media, and fully prototrophic strains could provide advantages in processes based on feedstocks whose preparation requires heating and/or acid treatment steps (e.g., lignocellulosic hydrolysates [13, 14]) that inactivate specific vitamins. In addition, processes based on vitamin-independent yeast strains may be less susceptible to contamination by vitamin-auxotrophic microorganisms such as lactic acid bacteria (15). Thus, chassis strains able to grow fast in the absence of single or multiple vitamins would therefore be of interest for industrial application. Moreover, engineering strategies aimed at enabling fast growth and product formation in the absence of single or multiple vitamins may be relevant for large-scale industrial application of *Saccharomyces* yeasts.

The goals of the present study were to investigate whether single-vitamin prototrophy of *S. cerevisiae* for inositol, nicotinic acid, pantothenic acid, *p*ABA, pyridoxine or thiamine could be achieved by ALE and to identify mutations that support fast growth in the absence of each of these vitamins. To this end, the laboratory strain *S. cerevisiae* CEN.PK113-7D was subjected to parallel aerobic ALE experiments that encompassed serial transfer in different synthetic media, which each lacked a single B vitamin. Independently evolved strains from each medium type were then characterized by whole-genome resequencing and the relevance of selected identified mutations was assessed by their reverse engineering in the parental non-evolved strain.

(This article was submitted to an online preprint archive [16].)

RESULTS

Assessment of CEN.PK113-7D specific B vitamin requirements. *S. cerevisiae* strains belonging to the CEN.PK lineage, which was developed in an interdisciplinary project supported by the German Volkswagen Stiftung between 1993 and 1994 (17), exhibit properties that make them good laboratory models for yeast biotechnology (18). To provide a baseline for ALE experiments, specific growth rates of the haploid strain CEN.PK113-7D were analyzed in aerobic batch cultures on complete synthetic medium with glucose (SMD) and on seven "SMDΔ" media from which either biotin, inositol, nicotinic acid, pantothenic acid, *p*ABA, pyridoxine, or thiamine was omitted. To limit interference by carryover of vitamins from precultures, specific growth rates were measured after a third consecutive transfer on each medium (Fig. 2A).

Consistent with the presence in its genome of genes predicted to encode all enzymes involved in biosynthetic pathways for all seven vitamins (Fig. 1 [5]), the strain CEN.PK113-7D grew on all SMDΔ versions. On complete SMD, a specific growth rate of 0.38 ± 0.02 h^{-1} was observed, while specific growth rates on SMDΔ lacking biotin, pantothenate, pyridoxine, thiamine, or inositol were 95%, 57%, 32%, 22%, or 19% lower, respectively. After three transfers, specific growth rates on SMDΔ lacking *p*ABA or nicotinic acid did not differ significantly from the specific growth rate on complete SMD (Fig. 2A). However, in SMDΔ lacking *p*ABA, growth in the first transfer was slower than in the first transfer on complete SMD (Fig. 2B). Extending the number of transfers to five, which corresponded to approximately 33 generations of selective growth, led to higher specific growth rates on several SMDΔ versions (Fig. 2A), suggesting that serial transfer selected for spontaneous faster-growing mutants.

Adaptive laboratory evolution of CEN.PK113-7D for fast growth in the absence of single vitamins. Serial transfer in independent triplicate aerobic shake-flask cultures on each SMDΔ version was used to select mutants that grew fast in the absence of individual vitamins. Specific growth rates of evolving populations were measured after 5, 10, 23, 38, and 50 transfers and compared to the specific growth rate of strain CEN.PK113-7D grown in complete SMD.

ALE experiments were stopped once the population reached a specific growth rate equal to or higher than 0.35 h^{-1}, which represents 90% to 95% of the specific growth rate of strain CEN.PK113-7D on complete SMD (Fig. 2A) (19–22). As already indicated by
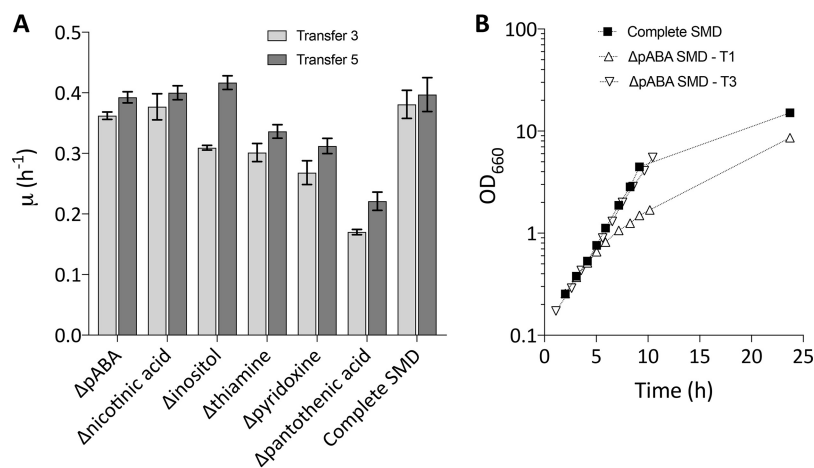
FIG 2 Specific growth rates of *S. cerevisiae* CEN.PK113-7D in aerobic batch cultures on complete SMD and on SMD lacking single vitamins. (A) Growth rate measurements were performed after 3 (light gray) and 5 (dark gray) consecutive transfers in the same medium. (B) Growth curves of CEN.PK113-7D in complete SMD (■) and at transfer 1 (△) and 3 (▽) in SMD lacking *para*-aminobenzoic acid (*p*ABA). In the latter medium, a lower specific growth rate was observed at transfer 1, but upon the third transfer, the growth rate was the same as in complete SMD. Error bars represent the standard deviations ($n = 9$ for complete SMD; $n = 3$ for all other media).

the specific growth rates observed after 3 and 5 transfers in SMDΔ (Fig. 2A), few transfers were required for reaching this target in SMDΔ lacking inositol, nicotinic acid, or *p*ABA. Conversely, more than 330 generations of selective growth were required to reach a specific growth rate of 0.35 h^{-1} on SMDΔ lacking either pantothenic acid, pyridoxine, or thiamine (Fig. 3A). At least two single-cell lines were isolated from each of the three independent ALE experiments on each SMDΔ version and the fastest growing single-cell line from each experiment was selected (strains IMS0724 to
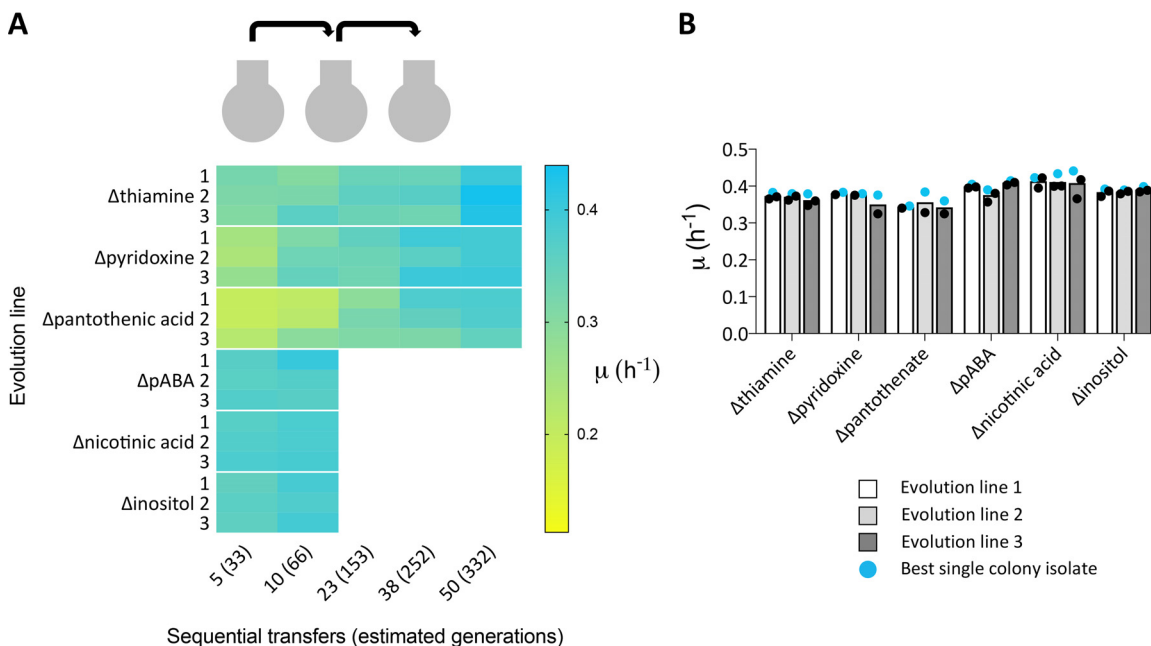
FIG 3 Heat map showing specific growth rates during ALE of *S. cerevisiae* CEN.PK113-7D on SMD lacking single vitamins. (A) Aerobic serial transfer experiments on each medium composition were performed in triplicates (rows). The specific growth rate of each evolving population was measured after a specific number of sequential transfers (columns). Yellow color indicates slow growth, while cyan indicates a specific growth rate statistically undistinguishable from that of the positive control (strain CEN.PK113-7D grown on SMD medium with all vitamins). (B) Specific growth rates of single-colony isolates from each independent biological replicate evolution line. The fastest-growing isolates, whose genomes were resequenced, are indicated in blue.

TABLE 1 Specific growth rates of best performing single-colony isolates obtained from serial transfer evolution experiments with *S. cerevisiae* CEN.PK113-7D on SMD and on SMD variants lacking individual B vitamins

Strain ID[a]	Evolution condition	Evolution replicate	Growth rate (h^{-1})	% improvement[b]
IMS0721	Complete SMD	1	0.443	17
IMS0722	Complete SMD	2	0.423	11
IMS0723	Complete SMD	3	0.419	10
IMS0747	No thiamine	1	0.383	35
IMS0748	No thiamine	2	0.379	30
IMS0749	No thiamine	3	0.379	38
IMS0736	No pyridoxine	1	0.383	45
IMS0737	No pyridoxine	2	0.379	44
IMS0738	No pyridoxine	3	0.376	48
IMS0733	No pantothenate	1	0.346	149
IMS0734	No pantothenate	2	0.384	155
IMS0735	No pantothenate	3	0.359	159
IMS0724	No nicotinic acid	1	0.423	4
IMS0725	No nicotinic acid	2	0.434	2
IMS0726	No nicotinic acid	3	0.441	2
IMS0730	No inositol	1	0.392	12
IMS0731	No inositol	2	0.389	24
IMS0732	No inositol	3	0.399	16
IMS0727	No pABA	1	0.405	6
IMS0728	No pABA	2	0.389	5
IMS0729	No pABA	3	0.414	4

[a]ID, identifier.
[b]Percentage improvement over the specific growth rate of the parental strain after three transfers in the same medium is also shown ($n = 1$ for each strain).

IMS0726 from SMDΔ lacking nicotinic acid, IMS0727 to IMS0729 from SMDΔ lacking *p*ABA, IMS0730 to IMS0732 from SMDΔ lacking inositol, IMS0733 to IMS0735 from SMDΔ lacking pantothenate, IMS0736 to IMS0738 from SMDΔ lacking pyridoxine, and IMS0747 to IMS0749 from SMDΔ lacking thiamine) (Table 1). The specific growth rates of isolates that had been independently evolved in each SMDΔ version did not differ by more than 6%. The largest difference (5.3%) was observed for isolates IMS0733 to IMS0735 evolved on SMDΔ lacking pantothenate (Fig. 3B).

Whole-genome sequencing of evolved strains and target identification. To identify mutations contributing to vitamin independence, the genomes of the sets of three independently evolved isolates for each SMDΔ version were sequenced with Illumina short-read technology. After aligning reads to the reference CEN.PK113-7D genome sequence (23), mapped data were analyzed for the presence of copy number variations (CNVs) and single nucleotide variations (SNVs) that occurred in annotated coding sequences.

A segmental amplification of 34 kb (from nucleotide 802500 to 837000) on chromosome VII, which harbors *THI4*, was observed in strain IMS0749 (Fig. 4A), which had been evolved in SMDΔ lacking thiamine. *THI4* encodes a thiazole synthase, a suicide enzyme that can only perform a single catalytic turnover (24). Segmental amplifications on chromosomes III and VIII were observed in strain IMS0725, which had been evolved in SMDΔ lacking nicotinic acid (Fig. 4B). Since these regions are known to be prone to recombination in the parental strain CEN.PK113-7D (23, 25), their amplification is not necessarily related to nicotinic acid independence.

SNV analysis was systematically performed, and data from the three sequenced isolates were compared. To eliminate false positives caused by mapping artifacts, reads of the CEN.PK113-7D strains were mapped back on its own reference assembly. Identified SNVs found were systematically subtracted. SNV analysis was restricted to non-synonymous mutations in coding sequences (Table 2).

In three of the six isolates from ALE experiments in SMDΔ lacking nicotinic acid or inositol, no non-synonymous SNVs were detected (Fig. 5). One strain (IMS0724) from a serial transfer experiment on SMDΔ lacking nicotinic acid showed SNVs in *RPG1* and *PMR1*, while a second strain (IMS0725) showed SNVs in *MTO1* and *VTH2*. A mutation in

A) CEN.PK113-7D vs IMS0749

THI4-ENP2-ECL1-NAT2-RPL24B-YGR149W-*CCM1*-RSR1-YGR153W-*GTO1-CYS4-PTI1-CHO2*
MTR3-NSR1-YGR160W-*RTS3*-YGR161W-C
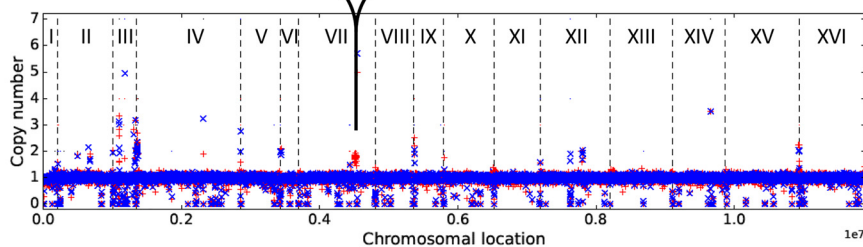
B) CEN.PK113-7D vs IMS0725
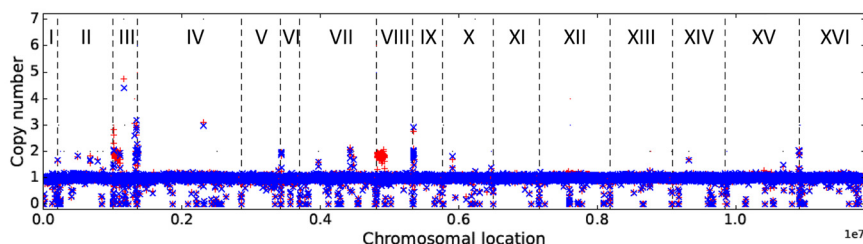
FIG 4 Read coverages across the chromosomes of evolved isolates IMS0725 evolved for nicotinic acid prototrophy (A) and IMS0749 evolved for thiamine prototrophy (B) (in red) compared to read coverage across the chromosomes of CEN.PK113-7D (in blue). Annotated genes found in the amplified region of IMS0749 are indicated.

YFR054W was identified in a single strain (IMS0730) evolved for inositol-independent growth. The absence of mutations in several strains subjected to serial transfer in SMDΔ lacking nicotinic acid or inositol is consistent with the fast growth of the parental strain CEN.PK113-7D in these media (Fig. 2A).

Sequencing of the three isolates evolved in SMDΔ lacking *p*ABA revealed only five SNVs, of which two were in *ABZ1* (strains IMS0727 and IMS0729) and one in *ARO7* (IMS0728), while SNVs in *NUP57* and *HTS2* were found in strains IMS0728 and IMS0729, respectively (Fig. 5). *NUP57* and *HTS2* could not be directly linked to *p*ABA metabolism. Conversely, Abz1 is an aminodeoxychorismate synthase that directs chorismate toward *p*ABA synthesis, and Aro7 is a chorismate mutase that catalyzes the first committed reaction toward phenylalanine and tyrosine and thereby diverts chorismate from *p*ABA synthesis (Fig. 1) (26, 27). These two SNVs therefore represented clear targets for reverse engineering (Table 2).

In line with the much longer ALE experiments (approximately 332 generations), strains evolved in SMDΔ lacking thiamine, pantothenate, or pyridoxine showed larger numbers of SNVs, with a maximum number of 30 SNVs in the isolate IMS0738 evolved in SMDΔ lacking pyridoxine (Table 2 and Fig. 5).

Evolution on SMDΔ lacking thiamine did not yield mutations that affected the same gene in all three independently evolved isolates. However, strains IMS0747 and IMS0749 shared SNVs in *CNB1* and *ERR3*. A third isolate, strain IMS0748, contained two SNVs in *PMR1* and *FRE2*. *CNB1*, *PMR1*, and *FRE2* all encode proteins that have been implicated in divalent cation homeostasis (28–32).

Isolates IMS0736 and IMS0737, which had been evolved in SMDΔ lacking pyridoxine, harbored only two and three mutations, respectively, while strain IMS0738 harbored 30 mutations. All three strains carried different mutated alleles of *BAS1*, which encodes a transcription factor involved in regulation of histidine and purine biosynthesis (33, 34). IMS0736 harbored a non-synonymous mutation causing an amino acid change position

TABLE 2 Non-conservative mutations found in single-colony isolates obtained from serial transfer evolution experiments with *S. cerevisiae* CEN.PK113-7D on SMD variants lacking individual B vitamins[a]

| Gene mutated in evolution expt	Codon change[b]	Amino acid change	Gene annotation
Pantothenate			
IMS0733			
AMN1	agC-agG	S67R	Antagonist of mitotic exit network protein 1
DAN4	aTc-aCc	I353T	Cell wall protein, delayed anaerobic 4
ERG3	Gct-Cct	A145P	Delta(7)-sterol 5(6)-desaturase, ergosterol biosynthesis 3
ERR3	ttG-ttT	L344F	Enolase-related protein 3
ISW2	**tCa-tGa**	**S181Stop**	**ISWI chromatin-remodeling complex ATPase, imitation switch subfamily 2**
IMS0734			
CDC15	Aca-Gca	T262A	Cell division control protein 15
RPS14A	Cca-Tca	P94S	40S ribosomal protein S14-A
TUP1	**gTg-gCg**	**V374A**	**General transcriptional corepressor**
RRT6	gCg-gTg	A267V	Regulator of rRNA gene transcription protein 6
CEG1	gCa-gTa	A4V	mRNA-capping enzyme subunit alpha
SCY1	Cct-Tct	P42S	Protein kinase-like protein SCY1
PDX1	gCa-gTa	A208V	Pyruvate dehydrogenase complex protein X component
TRM5	gCg-gTg	A106V	tRNA [guanine(37)-N1]-methyltransferase
GEF1	aGa-aTa	R637I	Anion/proton exchange transporter, glycerol ethanol, ferric requiring 1
LIP2	gGc-gAc	G235D	Octanoyltransferase
HFA1	Aag-Gag	K1021E	Acetyl coenzyme A carboxylase, mitochondrial
UBP8	aGt-aCt	S149T	Ubiquitin carboxyl-terminal hydrolase 8
MGS1	Cca-Aca	P392T	DNA-dependent ATPase
CPT1	Gtg-Atg	V255M	Cholinephosphotransferase 1
SPE2	**Gca-Aca**	**A278T**	***S*-Adenosylmethionine decarboxylase proenzyme**
GAL11	**aTt-aAt**	**I541N**	**Mediator of RNA polymerase II transcription subunit 15**
CUE5	Cca-Tca	P377S	Ubiquitin-binding protein
MIP1	Gca-Aca	A630T	DNA polymerase gamma
POC4	aGc-aTc	S7I	Proteasome chaperone 4
KAP120	tTg-tCg	L582S	Importin beta-like protein
KAP120	gAc-gGc	D850G	Importin beta-like protein
SEC16	Gca-Aca	A1015T	COPII coat assembly protein
IMS0735			
TUP1	**Cag-Tag**	**Q99Stop**	**General transcriptional corepressor**
FMS1	**Caa-Aaa**	**Q-33K**	**Polyamine oxidase**
GAL11	**Caa-Taa**	**Q383Stop**	**Mediator of RNA polymerase II transcription subunit 15**
Pyridoxine			
IMS0736			
BAS1	**cAa-cGa**	**Q152R**	**Myb-like DNA-binding protein, basal 1**
ERG5	Aga-Gga	R529G	C-22 sterol desaturase, ergosterol biosynthesis 5
IMS0737			
BAS1	Gat-Aat	D101N	Myb-like DNA-binding protein, basal 1
ERG5	Ggt-Tgt	G472C	C-22 sterol desaturase, ergosterol biosynthesis 5
IMS0738			
GIP4	Tcc-Ccc	S464P	GLC7-interacting protein 4
AOS1	Gtg-Atg	V286M	DNA damage tolerance protein RHC31
ORC4	aGt-aAt	S160N	Origin recognition complex subunit 4
MSB1	Att-Ttt	I180F	Morphogenesis-related protein, multicopy suppression of a budding defect 1
GCR2	Gga-Aga	G5R	Glycolytic genes transcriptional activator, glycolysis regulation 2
VNX1	aCa-aTa	T490I	Low-affinity vacuolar monovalent cation/H^+ antiporter
MMT1	gCt-gAt	A175D	Mitochondrial metal transporter 1
ISF1	Tat-Gat	Y220D	Increasing suppression factor 1
RPM2	Gcc-Acc	A1020T	Ribonuclease P protein component, mitochondrial
BAS1	**Tca-Cca**	**S41P**	**Myb-like DNA-binding protein, basal 1**
AAD14	agC-agA	S322R	Putative aryl-alcohol dehydrogenase AAD14
FAS1	gaA-gaT	E1829D	Fatty acid synthase subunit beta
BEM2	Aac-Cac	N792H	GTPase-activating protein, bud emergence 2/IPL2
APL1	gGt-gTt	G6V	AP-2 complex subunit beta
DPB11	agG-agT	R699S	DNA replication regulator, DNA polymerase B (II) 11
LSB6	Aca-Gca	T458A	Phosphatidylinositol 4-kinase, las seventeen binding protein 6
EFG1	aAa-aGa	K188R	rRNA-processing protein, exit from G$_1$ 1
CCH1	atG-atA	M828I	Calcium-channel protein 1
RNR4	Gca-Tca	A210S	Ribonucleoside-diphosphate reductase small chain 2
GCD2	tTa-tCa	L472S	Translation initiation factor eIF-2B subunit delta
YHR219W	aAt-aGt	N61S	Putative uncharacterized protein YHR219W

(Continued on next page)

TABLE 2 (Continued)

Gene mutated in evolution expt	Codon change[b]	Amino acid change	Gene annotation
CDC37	Gcc-Tcc	A275S	Hsp90 cochaperone, cell division cycle 37
SRP101	Gca-Aca	A75T	Signal recognition particle receptor subunit alpha homolog
ADE8	Gca-Aca	A142T	Phosphoribosylglycinamide formyltransferase
AIM9	gCa-gTa	A23V	Altered inheritance of mitochondria protein 9, mitochondrial
UTP20	tAt-tGt	Y1492C	U3 small nucleolar RNA-associated protein 20
RIF1	aGc-aTc	S1516I	Telomere length regulator protein, RAP1-interacting factor 1
PHO87	Gtc-Atc	V482I	Inorganic phosphate transporter
MAK21	tTg-tCg	L413S	Ribosome biogenesis protein, maintenance of killer 21
YDL176W	tCa-tAa	S186-Stop	Uncharacterized protein YDL176W
Thiamine			
IMS0747			
MAL12	Gtt-Ctt	V305L	Alpha-glucosidase, maltose fermentation 12
CNB1	**ttA-ttT**	**L82F**	**Calcineurin subunit B**
PRP16	aAa-aGa	K112R	Pre-mRNA-splicing factor ATP-dependent RNA helicase
ERR3	ttG-ttT	L447F	Enolase-related protein 3
IMS0748			
PMR1	**tCc-tAc**	**S104Y**	**Calcium-transporting ATPase 1**
FRE2	**aCt-aGt**	**T110S**	**Ferric/cupric reductase transmembrane component 2**
IMS0749			
YEL074W	cAc-cCc	H66P	Putative UPF0320 protein YEL074W
CNB1	**ttA-ttC**	**L82F**	**Calcineurin subunit B**
MSC1	Gtt-Att	V309I	Meiotic sister chromatid recombination protein 1
ERR3	ttG-ttT	L447F	Enolase-related protein 3
pABA			
IMS0727			
ABZ1	**cGt-cAt**	**R593H**	**Aminodeoxychorismate synthase**
IMS0728			
ARO7	**tTa-tCa**	**L205S**	**Chorismate mutase**
NUP57	tCc-tTc	S396F	Nucleoporin 57
IMS0729			
ABZ1	**cGt-cAt**	**R593H**	**Aminodeoxychorismate synthase**
HST2	ttG-ttT	L102F	NAD-dependent protein deacetylase, homolog of SIR two 2
Inositol			
IMS0730			
YFR045W	Gcc-Acc	A65T	Putative mitochondrial transport protein
IMS0732			
YFR045W	Gcc-Acc	A65T	Uncharacterized mitochondrial carrier
Nicotinic acid			
IMS0724			
RPG1	Ggt-Tgt	G294C	Eukaryotic translation initiation factor 3 subunit A
PMR1	Ggt-Agt	G694S	Calcium-transporting ATPase 1
IMS0725			
MTO1	atG-atT	M356I	Mitochondrial translation optimization protein 1
VTH2	Cca-Tca	P708S	Putative membrane glycoprotein, VPS10 homolog 2
VTH2	gTT-gCC	V478A	Putative membrane glycoprotein, VPS10 homolog 2
VTH2	TtT-GtG	F477V	Putative membrane glycoprotein, VPS10 homolog 2

[a]Mutations that were chosen for subsequent reverse engineering experiments are shown in boldface font. *S. cerevisiae* strains IMS0731 and IMS0726 evolved for fast *myo*-inositol- and nicotinic acid-independent growth, respectively, did not reveal non-conservative mutations and were not included in the table.
[b]Uppercase letters indicate the mutations.

152 (Q152R), while SNVs in strains IMS0737 and IMS0738 affected amino acids 101 (D101N) and 41 (S41P), respectively. Based on these results, *BAS1* was identified as priority target for reverse engineering.

Isolates IMS0733 and IMS0735, evolved on SMDΔ lacking pantothenic acid, carried three and five SNVs, respectively, while isolate IMS0734 carried 21 mutations. Isolates IMS0734 and IMS0735 both carried mutations in *TUP1* and *GAL11*, resulting in different single-amino acid changes (Tup1^{V374A} Gal11^{I541N} and Tup1^{Q99stop} Gal11^{Q383stop}, respectively). *TUP1* codes for a general transcriptional corepressor (35), while *GAL11* codes for a subunit of the tail of the mediator complex that regulates activity of RNA polymerase
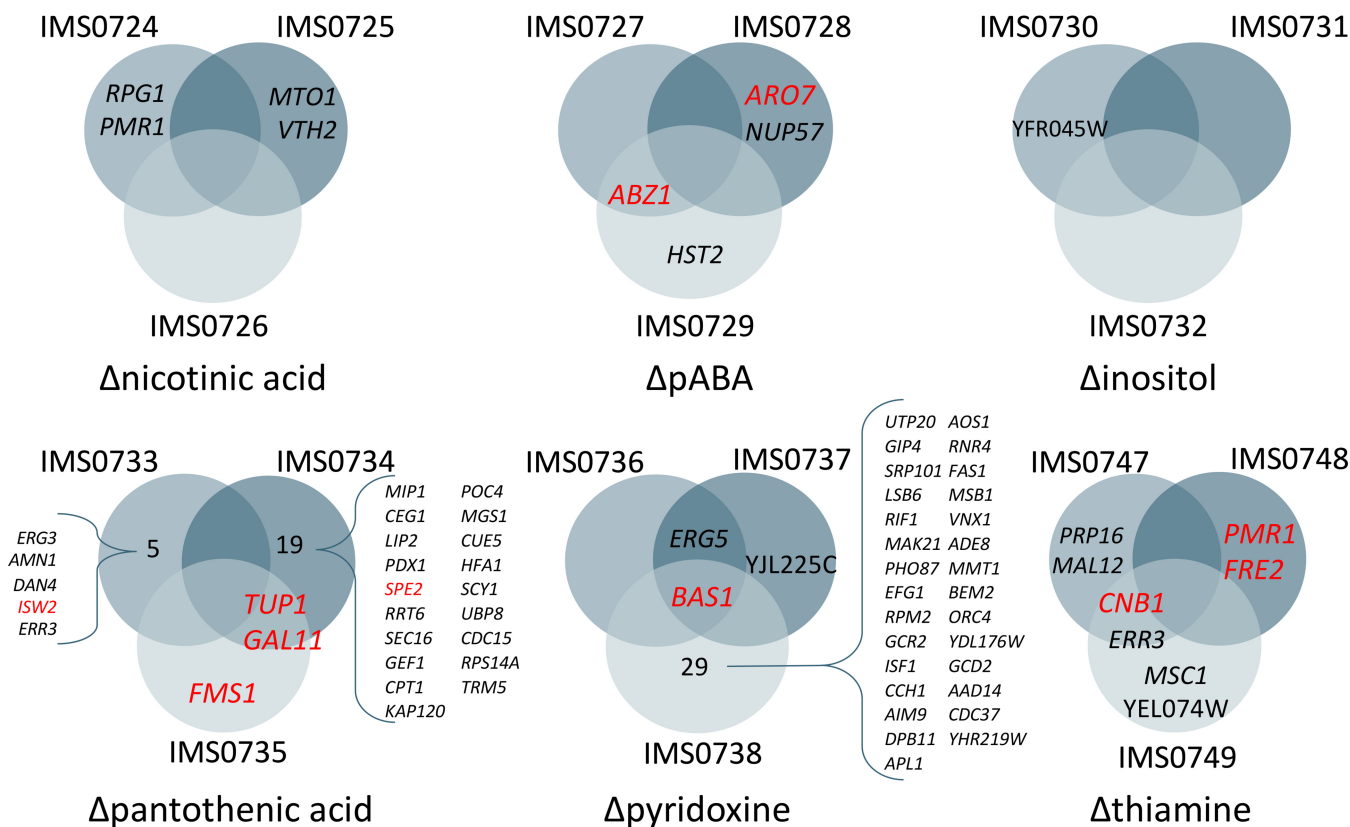
FIG 5 Venn diagrams showing non-synonymous mutations found in coding regions of isolated strains from the different evolution experiments. Each evolution experiment was performed in triplicates. The Venn diagrams show genes that acquired non-synonymous mutations in multiple independent evolution experiments for a specific medium as well as genes that were affected in a single replicate. Apparent mutations also found in the genome of the parent strain CEN.PK113-7D were subtracted and not shown. Target genes that were selected for reverse engineering are shown in red.

II (36). One of the mutations in strain IMS0733 affected *ISW2*, which encodes a subunit of the chromatin remodeling complex (37). These three genes involved in regulatory processes were selected for reverse engineering, along with *SPE2* and *FMS1*. The latter two genes, encoding *S*-adenosylmethionine decarboxylase (38) and polyamine oxidase (39), are directly involved in pantothenate biosynthesis and were found to be mutated in isolates IMS0734 and IMS0735, respectively.

In summary, based on mutations in the same gene in independently evolved isolates and/or existing information on involvement of affected genes in vitamin biosynthesis, mutations in 12 genes were selected for reconstruction in the parental strain CEN.PK113-7D. These were mutated alleles of *ISW2*, *GAL11*, *TUP1*, *FMS1*, and *SPE2* for pantothenate, in *BAS1* for pyridoxine, mutations in *CNB1*, *PMR1*, and *FRE2* as well as overexpression of *THI4* for thiamine, and mutations in *ABZ1* and *ARO7* for pABA. Since serial transfer on SMDΔ lacking nicotinic acid or inositol did not consistently yield mutations and the parental strain CEN.PK113-7D already grew fast on these media, no reverse engineering of mutations observed in isolates from those experiments was carried out.

Reverse engineering of target gene mutations and overexpression. To investigate whether the selected targets contributed to the phenotypes of the evolved strains, single point mutations or single-gene overexpression cassettes were introduced in a non-evolved reference strain, followed by analysis of specific growth rate in the relevant SMDΔ variant. For most target genes, a two-step strategy was adopted, so that a single-gene knockout mutant was constructed in the process (Fig. 6A and B). For the *SPE2* mutant strains IMX2308 and IMX2289, point mutations were introduced in a single step (Fig. 6C). The *THI4*-overexpressing strains IMX2290 and IMX2291 were constructed
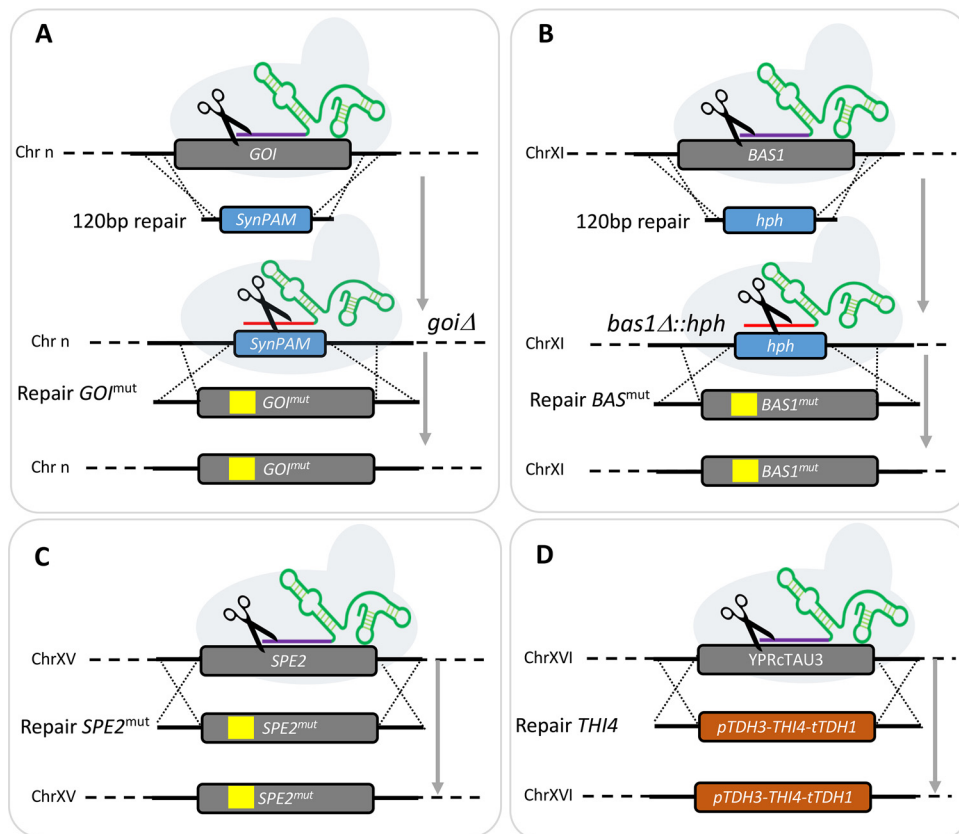
FIG 6 Strain construction strategies for reverse engineering. Most of the single mutation strains were generated in two steps. (A) First the gene of interest (GOI) was replaced by a synthetic 20-bp target sequence and 3-bp PAM sequence (SynPAM). In a second step, the SynPAM was targeted by Cas9 and substituted with the GOI mutant allele. (B) The SynPAM approach was not successful in targeting *BAS1*. For this reason, the *BAS1* mutant strains (IMX2135 to 2137) were constructed by first knocking out the gene by replacing it with the antibiotic marker hphNT1 that confers resistance to hygromycin. Then, in a second step, the selection marker was targeted with Cas9 and substituted with a *BAS1* mutant allele. (C) In the case of *SPE2* mutant strains (IMX2289 and IMX2308), the mutant allele was swapped with the wild-type (WT) allele in a single step. (D) The *THI4* overexpressing strains IMX2290 and IMX2291 were constructed by integrating a *THI4* overexpression cassette at the YPRcTau3 locus. SNVs are represented by yellow boxes.

by integrating the overexpression cassette at the YPRcTau3 locus (40) (Fig. 6D). Subsequently, multiple mutations that were found in strains evolved in the same SMDΔ version were combined into single engineered strains to test for additive or synergistic effects.

Thiamine. The specific growth rate of *S. cerevisiae* CEN.PK113-7D was only 27% lower in SMDΔ lacking thiamine than in complete SMD (Fig. 2A). Nevertheless, it took more than 300 generations of selective growth to obtain evolved isolates that compensated for this difference (Fig. 3 and Table 1). The role of mutations in *CNB1*, *FRE2*, and *PMR1* in this evolved phenotype was first investigated in the single knockout strains IMX1721, IMX1722, and IMX1723, respectively. While deletion of *PMR1* negatively affected the specific growth rate on SMDΔ lacking thiamine, deletion of either *CNB1* or *FRE2* resulted in a 17% increase of the specific growth rate on this medium relative to that of CEN.PK113-7D. However, strains IMX1721 (*cnb1Δ*) and IMX1722 (*fre2Δ*) still grew significantly slower than the evolved isolates (Fig. 7). Subsequently, the mutated alleles found in the evolved isolates were introduced at the native chromosomal locus, resulting in strains IMX1985 (*CNB1*^{L82F}), IMX1986 (*PMR1*^{S104Y}), and IMX1987 (*FRE2*^{T110S}). In addition, *THI4* was overexpressed (strain IMX2290) to simulate the copy number increase observed in IMS0749. Strains IMX1987 (*FRE2*^{T110S}) and IMX2290 (*THI4*↑) grew as fast as the evolved isolates on SMDΔ lacking thiamine (0.35 to
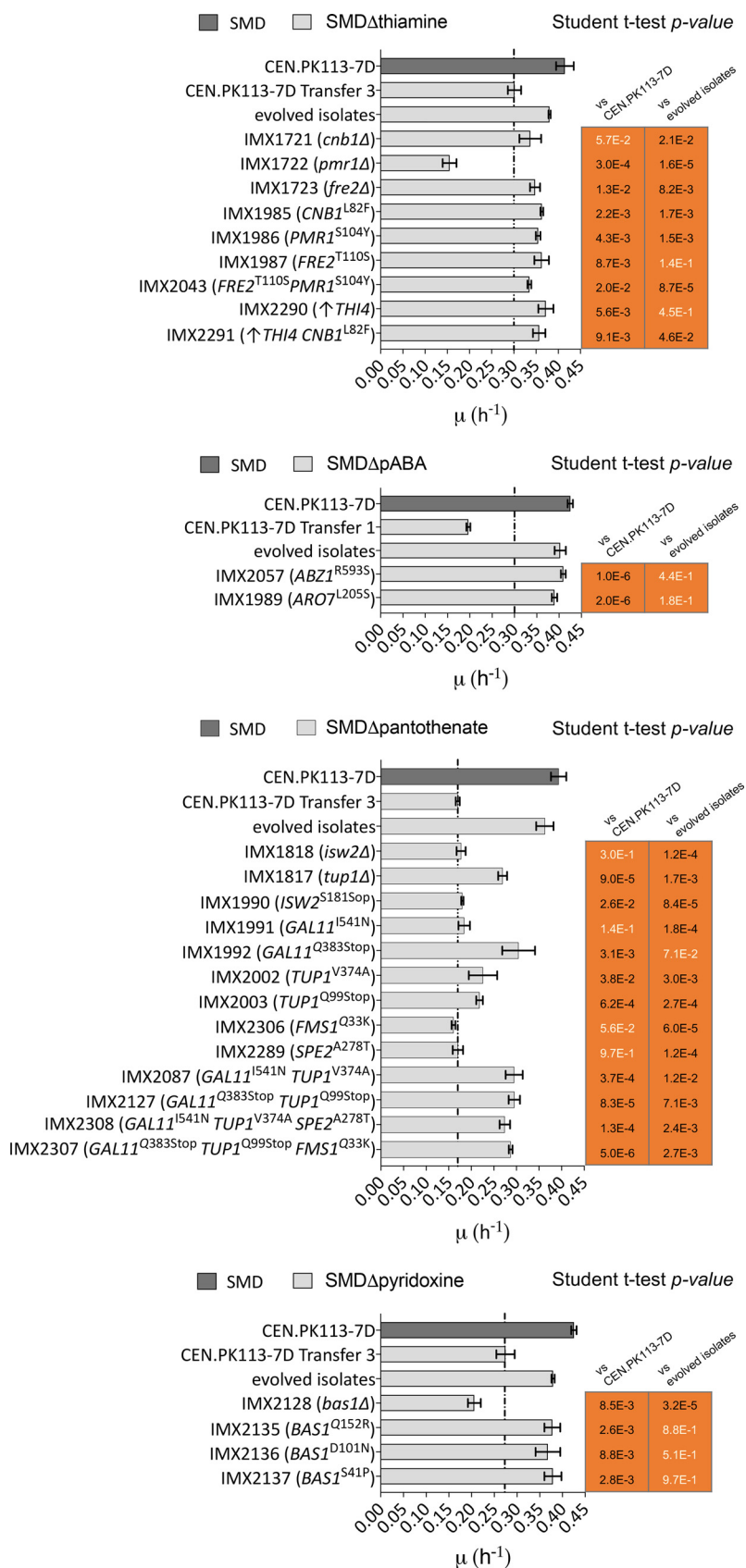
FIG 7 Specific growth rates of engineered *S. cerevisiae* strains carrying one or multiple gene deletions or reverse-engineered mutations in SMD media lacking thiamine (top), *p*ABA (second from top), pantothenic

(Continued on next page)

0.36 h^{-1}) (Fig. 7). Combination of these mutated alleles of *PMR1* and *FRE2*, which occurred together in isolate IMS0748, as well as of the two mutations resulting in growth improvement (*FRE2*^{T110S} and *THI4* ↑) was also tested. None of these combinations yielded a higher specific growth rate than observed in the evolved strains and in the reverse-engineered *FRE2*^{T110S} and *THI4* ↑ strains.

para-**Aminobenzoic acid.** In SMDΔ lacking *p*ABA, strain CEN.PK113-7D grew 50% slower than in complete SMD. However, it took only a few transfers to achieve fast *p*ABA-independent growth. The independently evolved isolates IMX2057 and IMX1989 harbored mutations affecting genes that encode chorismate-utilizing enzymes, the precursor of *p*ABA (*ABZ1*^{N593H} and *ARO7*^{L205S}, respectively) (Fig. 1). As these strains were able to grow in SMD without amino acid supplementation, these mutations did not cause a complete loss of function. However, they might well have affected the distribution of chorismate over *p*ABA and aromatic amino acid biosynthesis (26, 27). Introduction of either *ABZ1*^{N593H} or *ARO7*^{L205S}, while replacing the corresponding wild-type allele, eliminated the slower growth observed in strain CEN.PK113-7D during the first transfer on SMDΔ lacking *p*ABA. Specific growth rates of these reverse-engineered strains IMX2057 (*ABZ1*^{R593H}) and IMX1989 (*ARO7*^{L205S}) were not statistically different from those of the corresponding evolved isolates (Fig. 7).

Pantothenic acid. Omission of pantothenic acid from SMD led to a 57% lower specific growth rate of strain CEN.PK113-7D than observed in complete SMD (Fig. 2 and Table 1). Of a total number of 29 mutations found in three independently evolved isolates that showed fast growth in SMDΔ lacking pantothenate, SNVs in *ISW2*, *GAL11*, *TUP1*, *SPE2*, and *FMS1* were analyzed by reverse engineering. Single deletions of *SPE2*, *FMS1*, and *GAL11* resulted in an inability to grow on SMDΔ lacking pantothenate. This result was anticipated for the *spe2*Δ and *fms1*Δ mutants, in view of the roles of these genes in pantothenate biosynthesis. However, *GAL11* was not previously implicated in pantothenate biosynthesis. The *gal11*Δ strain was conditional, as the mutant did grow on complex yeast extract-peptone-dextrose (YPD) and SMD media. Of the remaining two deletion mutants, the *tup1*Δ strain IMX1817 showed a 68% higher specific growth rate on SMDΔ than strain CEN.PK113-7D, while deletion of *ISW2* did not result in faster growth on this medium (Fig. 7). Of seven SNVs that were individually expressed in the non-evolved strain background, only the *GAL11*^{Q383stop} mutation found in IMS0735 supported a specific growth rate of 0.33 h^{-1} on SMDΔ lacking pantothenate that was only 8% lower than that of the evolved isolates.

Combination of the *GAL11*^{Q383stop} mutation with *TUP1*^{Q99stop}, and *TUP1* with *FMS1*, did not lead to additional improvement, indicating that the *GAL11*^{Q383stop} mutation was predominantly responsible for the improved growth of evolved strain IMS0735 in the absence of pantothenate.

Pyridoxine. Strain CEN.PK113-7D grew 35% slower on SMDΔ lacking pyridoxine than on complete SMD (Fig. 2). Three different mutated alleles of *BAS1* were identified in strains that had been independently evolved for fast growth on the former medium (Fig. 3 and Table 2). Deletion, in a non-evolved reference strain, of *BAS1* (IMX2128) did not result in faster pyridoxine-independent growth (Fig. 7). Individual expression of the evolved *BAS1* alleles in strain IMX2128 yielded strains IMX2135 (*BAS1*^{Q152R}), IMX2136 (*BAS1*^{D101N}), and IMX2137 (*BAS1*^{S41P}). All three *BAS1* mutant strains grew faster on SMDΔ lacking pyridoxine than strain CEN.PK113-7D, reaching specific growth rates on this medium that were not significantly different from the average of those of evolved

FIG 7 Legend (Continued)
acid (middle), and pyridoxine (bottom). Specific growth rates of *S. cerevisiae* CEN.PK113-7D grown in complete SMD and evolved CEN.PK113-7D in SMD medium lacking the relevant vitamin are shown as references. The specific growth rate of strain CEN.PK113-7D in SMD medium lacking the relevant vitamin is shown and highlighted by a vertical line to help to visualize improved performance of engineered strains. Error bars represent the standard deviations ($n = 9$ for complete SMD, $n = 6$ for strain IMX1721; otherwise $n = 3$). A Student's *t* test was performed to compare the wild-type and evolved CEN.PK113-7D growth rate to the engineered strain growth rates, and non-significant differences are indicated with white letters (*P* value > 0.05).

strains IMS736, IMS737, and IMS738 (Fig. 7). These results suggest that *BAS1*, which was previously shown to be involved in regulation of purine and histidine biosynthesis (33, 34), may also be involved in regulation of pyridoxine biosynthesis in *S. cerevisiae*.

DISCUSSION

Vitamin requirements of *S. cerevisiae*. Most *S. cerevisiae* genomes harbor the full complement of genes required for synthesis of the seven B vitamins that are commonly included in chemically defined media for yeast cultivation (CDMY; for a recent review see references 5 and 10). Previous studies indicated that the presence of a complete set of biotin biosynthesis genes supported only slow growth on CDMY. The present study shows that, similarly, none of the other six B vitamins included in CDMY (inositol, nicotinic acid, pantothenic acid, *p*ABA, pyridoxine, and thiamine) are strictly required for growth. Remarkably, the impact of individually eliminating these six vitamins from glucose-containing CDMY differently affected specific growth rates in aerobic glucose-grown cultures, with growth rate reductions varying from 0% to 57%. It should, however, be noted that requirements for these growth factors, which for aerobic yeast cultivation cannot be formally defined as vitamins, and their absolute and relative requirements may well be condition and strain dependent. For example, it is well documented that synthesis of nicotinic acid and pantothenic acid by *S. cerevisiae* is strictly oxygen dependent (41). The data set compiled in the present study will, hopefully, serve as reference for investigating vitamin requirements of diverse natural isolates and laboratory and industrial strains and thereby help to obtain a deeper understanding of the genetics and ecology of vitamin prototrophy and vitamin biosynthesis in *S. cerevisiae*.

ALE and reverse engineering for identifying genes involved in fast B vitamin-independent growth. A serial transfer strategy was applied to select for spontaneous mutants that grew as fast in aerobic batch cultures on CDMY lacking either inositol, nicotinic acid, pyridoxine, thiamine, pantothenic acid, or *para*-aminobenzoic acid as in CDMY containing all these six vitamins as well as biotin. In the ALE experiments on media lacking nicotinic acid or inositol, fast growth was observed within a few cycles of batch cultivation, and not all fast-growing strains were found to contain mutations. These observations indicated that, under the experimental conditions, the native metabolic and regulatory network of *S. cerevisiae* was able to meet cellular requirements for fast growth in the absence of these "vitamins."

As demonstrated in other ALE studies, performing independent replicate evolution experiments helped in identifying biologically relevant mutations upon subsequent whole-genome sequencing (11, 12). The power of this approach is illustrated by the ALE experiments that selected for pyridoxine-independent growth, in which the independently evolved mutants IMS0736 and IMS0738 harbored 2 and 30 mutated genes, respectively, of which only *BAS1* also carried a mutation in a third independently sequenced isolate (Fig. 5 and Table 2).

In total, the role of 12 genes that were found to be mutated in the ALE experiments were selected for further analysis by reverse engineering of the evolved alleles and/or deletion mutations in the parental non-evolved genetic background (Fig. 5 and Table 2). These genes comprised three groups: (i) genes encoding enzymes known or inferred to be involved in the relevant vitamin synthesis pathway (*SPE2* and *FMS1* for pantothenate, *THI4* for thiamine, and *ABZ1* and *ARO7* for *p*ABA), (ii) genes encoding transcriptional regulator proteins (*TUP1* and *GAL11* for pantothenate and *BAS1* for pyridoxine), and (iii) non-transcriptional-regulator proteins whose functions were not previously associated with vitamin biosynthesis (*ISW2* for pantothenate and *CNB1*, *PMR1*, and *FRE2* for thiamine).

Of the first group of mutations defined above, only those in *SPE2* and *FMS1* were not found to contribute to faster growth in the absence of the relevant vitamin. The second group yielded interesting information on the regulation of vitamin biosynthesis in *S. cerevisiae*. In particular, the key role of mutations in *BAS1* in enabling fast pyridoxine-independent growth and the role of *GAL11* and *TUP1* mutations in fast pantothenate-
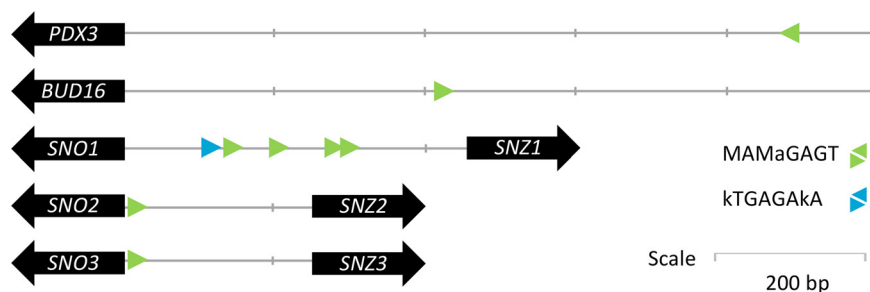
FIG 8 Schematic representation of Bas1 binding sites in promoter regions of genes involved in pyridoxal-5-phosphate biosynthesis. The two Bas1 consensus binding sequences MAMaGAGT and kTGAGAkA (75) are shown in green and blue, respectively.

independent growth dependency provided interesting insights and leads for further research.

The *S. cerevisiae* transcriptional activator Bas1 is involved in the regulation of purine and histidine (33, 34). Interestingly, Bas1 is also involved in the repression of genes involved in C_1 metabolism and of *SNZ1* (42). Snz1 is a subunit of a two-component pyridoxal-5′-phosphate synthase, which catalyzes the first step of the synthesis of pyridoxal-5-phosphate, the active form of pyridoxine in *S. cerevisiae* (43). Interrogation of the Yeastract database (44) for occurrence of transcription binding sites in promoter regions of pyridoxine biosynthesis genes confirmed the link already established between *BAS1* and *SNZ1* (42, 45). Moreover, this analysis revealed that all pyridoxine biosynthesis genes in *S. cerevisiae* contain a consensus Bas1 *cis*-regulatory binding motif (Fig. 8). Consistent with the regulatory role of Bas1 on *SNZ1* expression, Bas1 has been experimentally shown to repress transcription of genes involved in pyridoxine biosynthesis (46). The mutations found in *BAS1* may, therefore, have attenuated Bas1-mediated repression of pyridoxine biosynthetic genes and, thereby, enabled increased pyridoxine biosynthesis.

ALE experiments in pantothenate-free medium yielded different mutations in *TUP1* and *GAL11*, two major components of the yeast regulatory machinery. *TUP1* encodes a general transcriptional repressor that, in a complex with Cyc8, modifies chromatin structure such that genes are repressed (47–49). *GAL11* (also known as *MED15*) encodes a subunit of the mediator complex required for initiation by RNA polymerase II and consequently plays a critical role in transcription of a large number of RNA polymerase II-dependent genes (50, 51). Despite its involvement in general cellular transcriptional regulation, *GAL11* is not an essential gene for growth in complete medium (52). The inability of a *gal11Δ* strain to grow on glucose synthetic medium without pantothenate represents the first indication for a possible involvement of Gal11 in regulation of pantothenate metabolism. Gal11 interacts with transcriptional activators through various peptidic segments, including an N-terminal KIX domain. This region shows homology with the B-box motif found in the mammalian activating protein SRC-1 and is essential for recruitment of the mediator complex by other regulatory proteins (e.g., Gcn4) (53). Of two mutations found in *GAL11*, the most potent was a nonsense mutation at nucleotide 383. In contrast to a *gal11Δ* strain, a reverse-engineered strain carrying this premature stop codon grew on SMDΔ pantothenate, which indicates that the $GAL11^{Q383stop}$ allele encodes a functional peptide. Such a functional truncated Gal11 version was not previously described and is sufficiently long to include a complete KIX domain (AA_9 to AA_{86}) for recruitment of the RNA polymerase II machinery by an as yet unidentified transcription factor involved in regulation of pantothenate biosynthesis. Further research is required to resolve and understand the role of the wild-type and evolved alleles of *GAL11* in regulation of pantothenate metabolism.

A third group of non-transcription factor genes had not yet been associated with the biosynthesis of vitamins. Reverse engineering of a mutation in *ISW2*, which encodes an ATP-dependent DNA translocase involved in chromatin remodeling (54) identified in

the pantothenate evolution, did not yield a growth improvement. We cannot exclude that this mutation in association with *ERG3*, *AMN1*, *DAN4*, and *ERR3* identified in IMS0733 (Fig. 5 and Table 2) might have a significant impact, but systematic combinatorial analysis of the mutations was not performed.

Mutations in *CNB1*, *PMR1*, and *FRE2* identified in evolved isolates all improved growth of *S. cerevisiae* in the absence of thiamine (Fig. 7, top). These three genes all encode proteins involved in metal homeostasis: Fre2 is a ferric or cupric reductase (55), and Cnb1 is the regulatory B subunit of calcineurin, a Ca^{2+}/calmodulin-regulated type 2B protein phosphatase which regulates the nuclear localization of Crz1. This transcription factor influences the expression of a large number of genes. Its targets include *PMR1*, which encodes a high-affinity Ca^{2+}/Mn^{2+} P-type ATPase involved in Ca^{2+} and Mn^{2+} transport into the Golgi apparaus (30, 56). Neither of these three genes has hitherto been directly associated with thiamine. However, thiamine pyrophosphokinase (Thi80), thiamine phosphate synthase (Thi6), and hydroxymethylpyrimidine phosphate (Thi21 and Thi20) all require Mg^{2+} or Mn^{2+} as cofactors (57, 58). At low concentration, Mn^{2+} was shown to be a stronger activator of Thi80 than Mg^{2+} (59). In an ALE experiment with engineered xylose-fermenting assimilating *S. cerevisiae*, a nonsense mutation or deletion of *PMR1* caused selectively and strongly increased intracellular concentrations of Mn^{2+}, which was the preferred metal ion for the heterologously expressed *Piromyces* xylose isomerase (60). Although intracellular metal ion concentrations were not measured in the present study, the different phenotypes of a *pmr1*Δ deletion strain (IMX1722) and a *PMR1*^{S104Y} strain (IMX1986) (Fig. 7, top) indicate that the latter mutation does not act through a massive increase of the intracellular Mn^{2+} concentration.

In *S. cerevisiae*, synthesis of the thiazole moiety of thiamine biosynthesis involves sulfide transfer from an active-site cysteine (Cys205) residue of the thiazole synthase Thi4. This sulfur transfer reaction is iron dependent and generates inactive enzyme by formation of a dehydroalanine. Fe(II) plays an essential role in this sulfide transfer, which remains poorly understood (24). Further research is needed to investigate if the *FRE2* mutation in strain IMS0749 in some way increases the efficiency of the reaction catalyzed by the energetic single-turnover enzyme Thi4 and to resolve the role of metal homeostasis in vitamin biosynthesis.

Towards mineral media for cultivation of *S. cerevisiae*. With the exception of the carbon and energy sources for growth, B vitamins are the sole organic ingredients in standard CDMY recipes for aerobic cultivation of wild-type and industrial *S. cerevisiae* strains. In view of the chemical instability of some of these compounds, vitamin solutions cannot be autoclaved along with other medium components but are usually filter sterilized. In research laboratories and, in particular, in industrial processes, the costs, complexity, and contamination risks associated with the use of vitamins is significant. Complete elimination of vitamins from CDMY, without compromising specific growth rate, yield, or productivity, could therefore result in considerable cost and time savings as well as in improved standardization and robustness of cultivation procedures.

The present study demonstrates that, by ALE as well as introduction of small sets of defined mutations into *S. cerevisiae*, it is possible to achieve specific growth rates in single-vitamin-depleted CDMY that are close or identical to those found in CDMY supplemented with a complete vitamin mixture. While these results represent a first step toward the construction of prototrophic growth of *S. cerevisiae* and related yeasts, further research is required which trade-offs are incurred upon simultaneous introduction of the genetic interventions identified in this study and how they can be mitigated. This issue may be particularly relevant for mutations that affect genes involved in global regulation processes (51, 61), which may interfere with other cellular processes. In addition, simultaneous high-level expression of multiple enzymes with low-catalytic turnover numbers, with the suicide enzyme Thi4 (24, 62, 63) as an extreme example, may affect cell physiology due to the required resource allocation (64, 65).

In such cases, it may be necessary to expand metabolic engineering strategies beyond the native metabolic and regulatory capabilities of *S. cerevisiae* by expression of heterologous proteins and/or pathways with more favorable characteristics (66).

MATERIALS AND METHODS

Strains, media, and maintenance. The *S. cerevisiae* strains used and constructed in this study are shown in Table 3 and they all derive from the CEN.PK lineage (17, 67). Yeast strains were grown on synthetic medium with ammonium sulfate as a nitrogen source (SM) or YP medium (10 g/liter Bacto yeast extract, 20 g/liter Bacto peptone) as previously described (2). SM and YP media were autoclaved at 121°C for 20 min. Then, SM medium was supplemented with 1 ml/liter of filter-sterilized vitamin solution [0.05 g/liter D-(+)-biotin, 1.0 g/liter D-calcium pantothenate, 1.0 g/liter nicotinic acid, 25 g/liter *myo*-inositol, 1.0 g/liter thiamine hydrochloride, 1.0 g/liter pyridoxol hydrochloride, 0.20 g/liter 4-amino-benzoic acid]. Vitamin dropout media were prepared using vitamin solutions lacking either thiamine, pyridoxine, pantothenic acid, inositol, nicotinic acid, or *para*-aminobenzoic acid, yielding SMΔthiamine, SMΔpyridoxine, SMΔpantothenic acid, SMΔinositol, SMΔnicotinic acid, and SMΔpABA, respectively. A concentrated glucose solution was autoclaved at 110°C for 20 min and then added to the SM and YP media at a final concentration of 20 g/liter, yielding SMD and YPD, respectively. Five hundred-milliliter shake flasks containing 100 ml medium and 100-ml shake flasks containing 20 ml medium were incubated at 30°C and at 200 rpm in an Innova incubator (Brunswick Scientific, Edison, NJ). Solid media were prepared by adding 1.5% Bacto agar and, when indicated, 200 mg/liter G418 or 200 mg/liter hygromycin. *Escherichia coli* strains were grown in LB (10 g/liter Bacto tryptone, 5 g/liter Bacto yeast extract, 5 g/liter NaCl) supplemented with 100 mg/liter ampicillin or kanamycin. *S. cerevisiae* and *E. coli* cultures were stored at −80°C after the addition of 30% (vol/vol) glycerol.

Molecular biology techniques. PCR amplification of DNA fragments with Phusion Hot Start II high-fidelity polymerase (Thermo Scientific, Waltham, MA) and desalted or PAGE-purified oligonucleotide primers (Sigma-Aldrich, St. Louis, MO) was performed according to the manufacturers' instructions. DreamTaq polymerase (Thermo Scientific) was used for diagnostic PCR. Primers used in this study are shown in Table 4. PCR products were separated by gel electrophoresis using 1% (wt/vol) agarose gels (Thermo Scientific) in Tris-acetate-EDTA (TAE) buffer (Thermo Scientific) at 100 V for 25 min and purified either with a GenElutePCR Clean-Up kit (Sigma-Aldrich) or with a Zymoclean Gel DNA Recovery kit (Zymo Research, Irvine, CA). Plasmids were purified from *E. coli* using a Sigma GenElute Plasmid kit (Sigma-Aldrich). Plasmids used in this study are shown in Table 5. Yeast genomic DNA was isolated with the SDS-lithium acetate (LiAc) protocol (68). Yeast strains were transformed with the lithium acetate method (69). Four to eight single colonies were restreaked three consecutive times on selective media, and diagnostic PCRs were performed in order to verify their genotype. *E. coli* XL1-Blue was used for chemical transformation (70). Plasmids were then isolated and verified by either restriction analysis or by diagnostic PCR.

Laboratory evolution. Laboratory evolution of *S. cerevisiae* CEN.PK113-7D for fast growth in SMD medium lacking a single vitamin was performed by sequential transfer in aerobic shake-flask batch cultures. A frozen aliquot of strain CEN.PK113-7D was inoculated in a preculture shake flask containing SMD medium supplemented with all vitamins. Cells were then spun down, washed twice with sterile water, and used to inoculate a second shake flask containing SMD lacking one of the vitamins. The culture was then grown until stationary phase and transferred in a third shake flask containing the same fresh medium. At each transfer, 0.2 ml culture broth was transferred to 20 ml fresh medium, corresponding to approximately 6.7 generations in each growth cycle. The evolution experiment was performed in SMΔthiamine, SMΔpyridoxine, SMΔpantothenic acid, SMΔinositol, SMΔnicotinic acid, and SMΔpABA media. Each evolution experiment was performed in triplicates. After a defined number of transfers, intermediate strains were stocked and characterized for the growth rate. The experiment was stopped once the target specific growth rate of 0.35 h^{-1} was reached. From each evolved population, three single colonies were then isolated and stored. The specific growth rate of these single cell lines was measured to verify that they were representative of the evolved population. The best performing isolate from each evolution line was selected for whole-genome sequencing.

Shake flask growth experiments. For specific growth rate measurements of strains (evolved populations as well as single cell lines), an aliquot was used to inoculate a shake flask containing 100 ml of fresh medium. For specific growth rate measurements of the engineered strains, a frozen aliquot was thawed and used to inoculate a 20-ml starter culture that was then used to inoculate the 100-ml flask. An initial optical density at 660 nm (OD$_{660}$) of 0.1 or 0.2 was used as a starting point. The flasks were then incubated, and growth was monitored using a 7200 Jenway spectrometer (Jenway, Stone, United Kingdom). Specific growth rates were calculated from at least four time points in the exponential growth phase of each culture.

DNA sequencing. Genomic DNA of strains IMS0721, IMS0722, IMS0723, IMS0724, IMS0725, IMS0726, IMS0727, IMS0728, IMS0729, IMS0730, IMS0731, IMS0732, IMS0733, IMS0734, IMS0735, IMS0736, IMS0737, IMS0738, IMS0747, IMS0748, IMS0749, IMX2128, IMX2135, IMX2136, and IMX2137 was isolated with a Blood & Cell Culture DNA kit with 100/G Genomic-tips (Qiagen, Hilden, Germany) according to the manufacturer's protocol. Illumina-based paired-end sequencing with 150-bp reads was performed on 300-bp insert libraries (Novogene [HK] Company Limited, Hong Kong) with a minimum resulting coverage of 50×. Data mapping was performed against the CEN.PK113-7D genome (23) where an extra chromosome containing the relative integration cassette was previously added. Data processing and chromosome copy number variation determinations were conducted as previously described (60, 71).

TABLE 3 *Saccharomyces cerevisiae* strains used in this study

Strain ID	Relevant genotype or characteristic	Parental strain	Reference
CEN.PK113-7D	*MATa*		17
CEN.PK113-5D	*MATa ura3-52*		17
IMX585	*MATa can1Δ::cas9*-natNT2 U	CEN.PK113-7D	73
IMS0721	*MATa* evolved in SMD colony 1	CEN.PK113-7D	This study
IMS0722	*MATa* evolved in SMD colony 2	CEN.PK113-7D	This study
IMS0723	*MATa* evolved in SMD colony 3	CEN.PK113-7D	This study
IMS0724	*MATa* evolved in Δnicotinic acidSMD colony 1	CEN.PK113-7D	This study
IMS0725	*MATa* evolved in Δnicotinic acidSMD colony 2	CEN.PK113-7D	This study
IMS0726	*MATa* evolved in Δnicotinic acidSMD colony 3	CEN.PK113-7D	This study
IMS0727	*MATa* evolved in ΔpabaSMD colony 1	CEN.PK113-7D	This study
IMS0728	*MATa* evolved in ΔpabaSMD colony 2	CEN.PK113-7D	This study
IMS0729	*MATa* evolved in ΔpabaSMD colony 3	CEN.PK113-7D	This study
IMS0730	*MATa* evolved in ΔinositolSMD colony 1	CEN.PK113-7D	This study
IMS0731	Demonstrate evolved in ΔinositolSMD colony 2	CEN.PK113-7D	This study
IMS0732	*MATa* evolved in ΔinositolSMD colony 3	CEN.PK113-7D	This study
IMS0733	*MATa* evolved in Δpantothenic acidSMD colony 1	CEN.PK113-7D	This study
IMS0734	*MATa* evolved in Δpantothenic acidSMD colony 2	CEN.PK113-7D	This study
IMS0735	*MATa* evolved in Δpantothenic acidSMD colony 3	CEN.PK113-7D	This study
IMS0736	*MATa* evolved in ΔpyridoxineSMD colony 1	CEN.PK113-7D	This study
IMS0737	*MATa* evolved in ΔpyridoxineSMD colony 2	CEN.PK113-7D	This study
IMS0738	*MATa* evolved in ΔpyridoxineSMD colony 3	CEN.PK113-7D	This study
IMS0747	*MATa* evolved in ΔthiamineSMD colony 1	CEN.PK113-7D	This study
IMS0748	*MATa* evolved in ΔthiamineSMD colony 2	CEN.PK113-7D	This study
IMS0749	*MATa* evolved in ΔthiamineSMD colony 3	CEN.PK113-7D	This study
IMX1721	*MATa can1Δ::cas9*-natNT2 *cnb1Δ*::SynPAM	IMX585	This study
IMX1722	*MATa can1Δ::cas9*-natNT2 *pmr1Δ*::SynPAM	IMX585	This study
IMX1723	*MATa can1Δ::cas9*-natNT2 *fre2Δ*::SynPAM	IMX585	This study
IMX1817	*MATa can1Δ::cas9*-natNT2 *tup1Δ*::SynPAM	IMX585	This study
IMX1818	*MATa can1Δ::cas9*-natNT2 *isw2Δ*::SynPAM	IMX585	This study
IMX1819	*MATa can1Δ::cas9*-natNT2 *gal11Δ*::SynPAM	IMX585	This study
IMX1920	*MATa can1Δ::cas9*-natNT2 *aro7Δ*::SynPAM	IMX585	This study
IMX1985	*MATa can1Δ::cas9*-natNT2 SynPAMΔ::*CNB1*^{L82F}	IMX1721	This study
IMX1986	*MATa can1Δ::cas9*-natNT2 SynPAMΔ::*PMR1*^{S104Y}	IMX1722	This study
IMX1987	*MATa can1Δ::cas9*-natNT2 SynPAMΔ::*FRE2*^{T110S}	IMX1723	This study
IMX1988	*MATa can1Δ::cas9*-natNT2 *abz1Δ*::SynPAM	IMX585	This study
IMX1989	*MATa can1Δ::cas9*-natNT2 SynPAMΔ::*ARO7*^{L205S}	IMX1920	This study
IMX1990	*MATa can1Δ::cas9*-natNT2 SynPAMΔ::*ISW2*^{S181stop}	IMX1818	This study
IMX1991	*MATa can1Δ::cas9*-natNT2 SynPAMΔ::*GAL11*^{I541N}	IMX1819	This study
IMX1992	*MATa can1Δ::cas9*-natNT2 SynPAMΔ::*GAL11*^{Q383stop}	IMX1819	This study
IMX2002	*MATa can1Δ::cas9*-natNT2 SynPAMΔ::*TUP1*^{V374A}	IMX1817	This study
IMX2003	*MATa can1Δ::cas9*-natNT2 SynPAMΔ::*TUP1*^{Q99stop}	IMX1817	This study
IMX2043	*MATa can1Δ::cas9*-natNT2 SynPAMΔ::*FRE2*^{T110S} *pmr1Δ*::*PMR1*^{S104Y}	IMX1986	This study
IMX2057	*MATa can1Δ::cas9*-natNT2 SynPAMΔ::*ABZ1*^{R593H}	IMX1988	This study
IMX2066	*MATa can1Δ::cas9*-natNT2 SynPAMΔ::*TUP1*^{V374A} *gal11Δ*::SynPAM	IMX2002	This study
IMX2110	*MATa can1Δ::cas9*-natNT2 SynPAMΔ::*GAL11*^{Q383stop} *tup1Δ*::SynPAM	IMX1992	This study
IMX2127	*MATa can1Δ::cas9*-natNT2 SynPAMΔ::*GAL11*^{Q383stop} SynPAMΔ::*TUP1*^{Q99stop}	IMX2110	This study
IMX2128	*MATa can1Δ::cas9*-natNT2 *bas1Δ*::hphNT1	IMX585	This study
IMX2087	*MATa can1Δ::cas9*-natNT2 SynPAMΔ::*TUP1*^{V374A} SynPAMΔ::*GAL11*^{I541N}	IMX2066	This study
IMX2135	*MATa can1Δ::cas9*-natNT2 hphNT1Δ::*BAS1*^{Q152R}	IMX2128	This study
IMX2136	*MATa can1Δ::cas9*-natNT2 hphNT1Δ::*BAS1*^{D101N}	IMX2128	This study
IMX2137	*MATa can1Δ::cas9*-natNT2 hphNT1Δ::*BAS1*^{S41P}	IMX2128	This study
IMX2290	*MATa can1Δ::cas9*-natNT2 YPRcTau3::*pTDH3-THI4-tTDH*1	IMX585	This study
IMX2291	*MATa can1Δ::cas9*-natNT2 SynPAMΔ::*CNB1*^{L82F} YPRcTau3::*pTDH3-THI4-tTDH*1	IMX1985	This study
IMX2289	M*MATa* ATa *can1Δ::cas9*-natNT2 *SPE2*^{A278T}	IMX585	This study
IMX2292	*MATa can1Δ::cas9*-natNT2 *fms1Δ*::SynPAM	IMX585	This study
IMX2306	M*MATa* ATa *can1Δ::cas9*-natNT2 SynPAMΔ::*FMS1*^{Q33K}	IMX2292	This study
IMX2308	*MATa can1Δ::cas9*-natNT2 SynPAMΔ::*GAL11*^{Q383stop} SynPAMΔ::*TUP1*^{V374A} *SPE2*^{A278T}	IMX2127	This study
IMX2294	*MATa can1Δ::cas9*-natNT2 SynPAMΔ::*TUP1*^{V374A} SynPAMΔ::*GAL11*^{I541N} *FMS1*^{Q33K}::SynPAM	IMX2087	This study
IMX2307	*MATa can1Δ::cas9*-natNT2 SynPAMΔ::*TUP1*^{V374A} SynPAMΔ::*GAL11*^{I541N} SynPAMΔ::*FMS1*^{Q33K}	IMX2294	This study

Plasmid cloning. Plasmids carrying two copies of the same genomic RNA (gRNA) were cloned by *in vitro* Gibson assembly as previously described (72). In brief, an oligonucleotide carrying the 20-bp target sequence and homology to the backbone plasmid was used to amplify the fragment carrying the 2-μm origin of replication sequence by using pROS13 as the template. The backbone linear fragment was amplified by using primer 6005 and either pROS12 or pROS13 as the template (73). The two fragments were then gel purified, combined, and assembled *in vitro* using the NEBuilder HiFi DNA Assembly master

TABLE 4 Oligonucleotide primers used in this study

Primer ID	Sequence	Product(s)[a]
6005	GATCATTTATCTTTCACTGCGGAGAAG	gRNA pROS plasmid backbone amplification
6006	GTTTTAGAGCTAGAAATAGCAAGTTAAAATAAGGCTAGTC	gRNA pROS plasmid backbone amplification
14229	TGCGCATGTTTCGGCGTTCGAAACTTCTCCGCAGTGAAAGATAAATGATCAGTAGAATTTCACCTAGACG GTTTTAGAGCTAGAAATAGCAAGTTAAAATAAG	2-μm fragment for SynPAM gRNA plasmid
13686	TGCGCATGTTTCGGCGTTCGAAACTTCTCCGCAGTGAAAGATAAATGATCCTGCGGTGATAGAACCCTG GGTTTTAGAGCTAGAAATAGCAAGTTAAAATAAG	2-μm fragment for *ABZ1* gRNA plasmid
14988	CTTTTACACGATGACCTTTCGAGATTTCACAAGGGGGATAAAGGAAGTAGAATTTCACCTAGACGTGGA TATTTGTATATTATTAGATATGTATGCAAACATTTTCTTTAGAA	*ABZ1* KO repair oligonucleotide
14989	TTCTAAAGAAAATGTTTGCATACATATCTAATAATATACAAATATCCACGTCTAGGTGAAATTCTACTTC CTTTATCCCCCTTGTGAAATCTCGAAAGGTCATCGTGTAAAAG	*ABZ1* KO repair oligonucleotide
13693	AAAACCGCGAATATATAAAAACAAGC	*ABZ1* mutant allele amplification
13694	GGCACAAAACGTCATTTTCC	*ABZ1* mutant allele amplification
15075	TAATCACTCGGCAATGTGGAATTGTTACCGTGATAGCCTTCATGCAGTAGAATTTCACCTAGACGTGGAT CTTATACCAATTTTATGCAGGATGCTGAGTGCTATTTGTTAGC	*ARO7* KO repair oligonucleotide
15076	GCTAACAAATAGCACTCAGCATCCTGCATAAAATTGGTATAAGATCCACGTCTAGGTGAAATTCTACTGC ATGAAGGCTATCACGGTAACAATTCCACATTGCCGAGTGATTA	*ARO7* KO repair oligonucleotide
12052	CAGGAGTCTCTGAGCAAGGC	*ARO7* mutant allele amplification
12053	ACCATGCTAAGAGCTGCTCC	*ARO7* mutant allele amplification
15037	TGCGCATGTTTCGGCGTTCGAAACTTCTCCGCAGTGAAAGATAAATGATCAGCATCAGAAGTAATAAC AAGTTTTAGAGCTAGAAATAGCAAGTTAAAATAAG	2-μm fragment for *BAS1* gRNA plasmid
15584	AAACTTTTGTTGTAGCGTTTTTGCTTTTTTTTTTTATCGCAGAATACATTTTATCGAGATAGGTCTAGAG ATCTGTTTAGCTTGC	Repair fragment with hphNT1 for *BAS1* KO
15585	ATTACAAAACTAATATGTTAAACAATTGAAAGATTTGTGTTTTTTTTCGGCCTTGCCTTCAGCTCCAGCT TTTGTTCCC	Repair fragment with hphNT1 for *BAS1* KO
13687	CCTTTGACGATGTGCAACGG	Amplification *BAS1* mutant allele
13688	AACGCCCTTTGTGTTTGTGG	Amplification *BAS1* mutant allele
13520	TGCGCATGTTTCGGCGTTCGAAACTTCTCCGCAGTGAAAGATAAATGATCTCTTGCTGGACGTATAATGG GTTTTAGAGCTAGAAATAGCAAGTTAAAATAAG	2-μm fragment for *CNB1* gRNA plasmid
13612	ACTCAATGGTGATCAGAATCCATAGAAGCATTTTTATTTCTTAAAAGTAGAATTTCACCTAGACGTGGGA CTAGGGACACTTCATTCATTTATGGTATGCCAATATTTTTAA	*CNB1* KO repair oligonucleotide
13613	TTAAAAATATTGGCATACCATAAATGAATGAAGTGTCCCCTAGTCCCACGTCTAGGTGAAATTCTAC TTTTAAGAAATAAAAATGCTTCTATGGATTCTGATCACCATTGAGT	*CNB1* KO repair oligonucleotide
13523	GCATCAGCACTGCAGAATCG	*CNB1* mutant allele amplification
13524	GATCCCCCTTTGTGCATTGC	*CNB1* mutant allele amplification
13521	TGCGCATGTTTCGGCGTTCGAAACTTCTCCGCAGTGAAAGATAAATGATCCATAAAAAGAGAGACCAC TGGTTTTAGAGCTAGAAATAGCAAGTTAAAATAAG	2-μm fragment for *PMR1* gRNA plasmid
13541	CCAGCACAGACGTAAGCTTAAGTGTAAGTAAAAGATAAGATAATTAGTAGAATTTCACCTAGACGTGG TATGTCACATTTTGTGCTTTTATCGTTTTTCCTTCCTTCCCTTTA	*PMR1* KO repair oligonucleotide
13542	TAAAGGGAAGGAAGGAAAAACGATAAAAGCACAAAATGTGACATACCACGTCTAGGTGAAATTCTAC TAATTATCTTATCTTTTACTTACACTTAAGCTTACGTCTGTGCTGG	*PMR1* KO repair oligonucleotide
11292	TCGCCCCGTTCTTTCCATTC	*PMR1* mutant allele amplification
11293	GGGCGAAAAGGTAAGAACGC	*PMR1* mutant allele amplification
13522	TGCGCATGTTTCGGCGTTCGAAACTTCTCCGCAGTGAAAGATAAATGATCCATAAAAGAACATTGCAC CAGTTTTAGAGCTAGAAATAGCAAGTTAAAATAAG	2-μm fragment for *FRE2* gRNA plasmid
13539	AATAAAGTCTTTTTTATCCAAAGCTTATGAAACCCAACGAATATAAGTAGAATTTCACCTAGACGTG GTCATTTTTTACTTAAAACTAGTCATTTCATTAATAATACCTATCC	*FRE2* KO repair oligonucleotide
13540	GGATAGGTATTATTAATGAAATGACTAGTTTTAAGTAAAAAATGACCACGTCTAGGTGAAATTCTACTTA TATTCGTTGGGTTTCATAAGCTTTGGATAAAAAAGACTTTATT	*FRE2* KO repair oligonucleotide
13524	GATCCCCCTTTGTGCATTGC	*FRE2* mutant allele amplification
13525	TGGCTCAATGATGCTAGTGGG	*FRE2* mutant allele amplification
12174	GCATCGTCTCATCGGTCTCATATGTCTGCTACCTCTACTGCTACTTCC	*THI4* with YTK part 3 compatible overhangs
12175	ATGCCGTCTCAGGTCTCAGGATCTAAGCAGCAAAGTGTTTCAAAATTTG	*THI4* with YTK part 3 compatible overhangs
14586	ACAGTTTTGACAACTGGTTACTTCCCTAAGACTGTTTATATTAGGATTGTCAAGACACTCCAGTTCGAGT TTATCATTATCAATAC	*THI4*↑ cassette repair for integration
14587	ATAATTATAATATCCTGGACACTTTACTTATCTAGCGTATGTTATTACTCGATAAGTGCTCGTTCAGGGT AATATATTTTAACC	*THI4*↑ cassette repair for integration
13518	TGCGCATGTTTCGGCGTTCGAAACTTCTCCGCAGTGAAAGATAAATGATCTGAATCTGGTGATAGCACCG GTTTTAGAGCTAGAAATAGCAAGTTAAAATAAG	2-μm fragment for *GAL11* gRNA plasmid

(Continued on next page)

TABLE 4 (Continued)

Primer ID	Sequence	Product(s)[a]
13533	TACTCAAAGATCAAGGATTAAAACGCTATTTCTTTTAAATCTGCTAGTAGAATTTCACCTAGACGTGGACATTTGAAGTTTCCATACTTTTGATACTTTTGAAGTTACTTCGT	*GAL11* KO repair oligonucleotide
13534	ACGAAGTAACTTCAAAAGTATCAAAAGTATGGAAACTTCAAATGTCCACGTCTAGGTGAAATTCTACTAGCAGATTTAAAAGAAATAGCGTTTTAATCCTTGATCTTTGAGTA	*GAL11* KO repair oligo
13498	TTCGAATCGGGGCCTTCCTTC	*GAL11* mutant allele amplification
13499	TGCTTGAAGTGGCACTTTGC	*GAL11* mutant allele amplification
13517	TGCGCATGTTTCGGCGTTCGAAACTTCTCCGCAGTGAAAGATAAATGATCTGGAAGGGTAGACCATGACAGTTTTAGAGCTAGAAATAGCAAGTTAAAATAAG	2-μm fragment for *TUP1* gRNA plasmid
13531	TGATAAGCAGGGGAAGAAAGAAATCAGCTTTCCATCCAAACCAATAGTAGAATTTCACCTAGACGTGGGAACAGAACACAAAAGGAACACTTTACAAATGTAACTAACTAAAC	*TUP1* KO repair oligonucleotide
13532	GTTTAGTTAGTTACATTTGTAAAGTGTTCCTTTTGTGTTCTGTTCCCACGTCTAGGTGAAATTCTACTATTGGTTTGGATGGAAAGCTGATTTCTTTCTTCCCCTGCTTATCA	*TUP1* KO repair oligonucleotide
15077	CACGCCAAGTTACCTTTCGC	*TUP1* mutant allele amplification
15078	GGAAGGGATGAATGGTGAGG	*TUP1* mutant allele amplification
13519	TGCGCATGTTTCGGCGTTCGAAACTTCTCCGCAGTGAAAGATAAATGATCGAAAAGAGAAGGCAAAACGGTTTTAGAGCTAGAAATAGCAAGTTAAAATAAG	2-μm fragment for *ISW2* gRNA plasmid
13535	CTTGTTGGTTTAAGTCGTAACAAAAGGAAAACTTACAATCAGATCAGTAGAATTTCACCTAGACGTGGATCATGTATTGTGCATTAAAATAAGTGACGTGAGAGATATAATTT	*ISW2* KO repair oligonucleotide
13536	AAATTATATCTCTCACGTCACTTATTTTAATGCACAATACATGATCCACGTCTAGGTGAAATTCTACTGATCTGATTGTAAGTTTTCCTTTTGTTACGACTTAAACCAACAAG	*ISW2* KO repair oligonucleotide
13496	TCACCCAGAGGCAAAAGGTG	*ISW2* mutant allele amplification
13497	TAGTTAAAGCGGCTCGACCC	*ISW2* mutant allele amplification
16598	TGCGCATGTTTCGGCGTTCGAAACTTCTCCGCAGTGAAAGATAAATGATCTCAAGATTGTCTTGTTCTTGGTTTTAGAGCTAGAAATAGCAAGTTAAAATAAGGCTAGTCCGTTATCAAC	2-μm fragment for *FMS1* gRNA plasmid
13527	AACAAGAAGTGAGTTAATAAAGGCAAAAACAGTGGTCGTGTGAGAAGTAGAATTTCACCTAGACGTGGAATCTATTTTTTCGAAATTACTTACACTTTTGACGGCTAGAAAAG	*FMS1* KO repair oligonucleotide
13528	CTTTTCTAGCCGTCAAAAGTGTAAGTAATTTCGAAAAAATAGATTCCACGTCTAGGTGAAATTCTACTTCTCACACGACCACTGTTTTTGCCTTTATTAACTCACTTCTTGTT	*FMS1* KO repair oligonucleotide
13525	TGGCTCAATGATGCTAGTGGG	*FMS1* mutant allele amplification
13526	AGCCAAATTGCCAAGAAAGGG	*FMS1* mutant allele amplification
16601	TGCGCATGTTTCGGCGTTCGAAACTTCTCCGCAGTGAAAGATAAATGATCGCGTGAACGCAAATGCATCGGTTTTAGAGCTAGAAATAGCAAGTTAAAATAAGGCTAGTCCGTTATCAAC	2-μm fragment for *SPE2* gRNA plasmid
16602	AATAGTATTTTTCAGCGAGAATCATATTGGATGAGTATCCACATGGCGTGAACGCAAATGtATCGTGaTGAAATGATAAATCGGAGTCTTGGGCCGAGTTGACATATATTTCGTCAAG	*SPE2* mutation-carrying repair oligonucleotide
16603	CTTGACGAAATATATGTCAACTCGGCCCAAGACTCCGATTTATCATTTCAtCACGATaCATTTGCGTTCACGCCATGTGGATACTCATCCAATATGATTCTCGCTGAAAAATACTATT	*SPE2* mutation-carrying repair oligonucleotide
12174	GCATCGTCTCATCGGTCTCATATGTCTGCTACCTCTACTGCTACTTCC	YTK-compatible end addition to *THI4* CDS
12175	ATGCCGTCTCAGGTCTCAGGATCTAAGCAGCAAAGTGTTTCAAAATTTG	YTK-compatible end addition to *THI4* CDS
12985	TGCGCATGTTTCGGCGTTCGAAACTTCTCCGCAGTGAAAGATAAATGATCAAACATTCAAATATATTCCAGTTTTAGAGCTAGAAATAGCAAGTTAAAATAAG	2-μm fragment for YPRcTau3 gRNA plasmid
13261	AATACGAGGCGAATGTCTAGG	*THI4* integration check
13262	GCCTCCCCTAGCTGAACAAC	*THI4* integration check
13492	TACAGCTCGCTCCTTGCATC	*SPE2* mutation check
13493	GCTTGCTTGGAGGGCTTTTC	*SPE2* mutation check

[a]KO, knockout.

mix (New England BioLabs, Ipswich, MA) according to the manufacturer's instructions. Transformants were selected on LB plates supplemented with 100 mg/liter ampicillin.

Primers 13520, 13521, 13522, 13686, 13518, 14229, 13517, 13519, 15037, 15728, 12985, 16598, and 16601 were used to amplify the 2-μm fragments targeting *CNB1*, *PMR1*, *FRE2*, *ABZ1*, *GAL11*, SynPAM, *TUP1*, *ISW2*, *BAS1*, hphNT1, YPRcTau3, *FMS1*, and *SPE2*, respectively. The fragment targeting *GAL11* was cloned in a pROS12 backbone yielding plasmid pUDR441. The fragments targeting *CNB1*, *PMR1*, *FRE2*, *ABZ1*, SynPAM, *TUP1*, *ISW2*, *BAS1*, hphNT1, YPRcTau3, *FMS1*, and *SPE2* were cloned in a pROS13 backbone yielding plasmids pUDR388, pUDR389, pUDR390, pUDR438, pUDR471, pUDR472, pUDR473, pUDR566, pUDR592, pUDR514, pUDR652, and pUDR651, respectively.

The plasmid carrying the expression cassette for *THI4* was cloned by golden gate assembly using the yeast toolkit (YTK) parts (74). The *THI4* coding sequence was amplified using the primer pair 12174/12175 and CEN.PK113-7D genomic DNA as a template in order to add YTK compatible ends to the gene. The PCR product was then purified and combined together with plasmids pYTK009, pYTK056, and pYTK096 in a BsaI golden gate reaction that yielded plasmid pUDI180.

Strain construction. Strains carrying the target mutations were all constructed starting from IMX585 expressing the Cas9 protein (73). For all strain except for IMX2290, IMX2291, IMX2289, and IMX2308, a

TABLE 5 Plasmids used in this study

Plasmid	Relevant characteristics	Reference
pROS12	colE1^{ori} 2-μm *bla* hphNT1 gRNA-CAN1.Y gRNA-ADE2.Y	11
pROS13	colE1^{ori} 2-μm *bla aph* gRNA-*CAN1*.Y gRNA-*ADE2*.Y	11
pUDR412	colE1^{ori} 2-μm *bla* hphNT1 gRNA-ARO7 gRNA-ARO7	19
pYTK009	colE1^{ori} *cat pTDH3*	74
pYTK056	colE1^{ori} *cat tTDH1*	74
pYTK096	colE1^{ori} *aph URA3* 5′ homology *sfGFP URA3 URA3* 3′ homology	74
pUDR388	colE1^{ori} 2-μm *bla aph* gRNA-*CNB1* gRNA-*CNB1*	This study
pUDR389	colE1^{ori} 2-μm *bla aph* gRNA-PMR1 gRNA-PMR1	This study
pUDR390	colE1^{ori} 2-μm *bla aph* gRNA-FRE2 gRNA-FRE2	This study
pUDR438	colE1^{ori} 2-μm *bla aph* gRNA-ABZ1 gRNA-ABZ1	This study
pUDR441	colE1^{ori} 2-μm *bla* hphNT1 gRNA-GAL11 gRNA-GAL11	This study
pUDR471	colE1^{ori} 2-μm *bla aph* gRNA-SynPAM gRNA-SynPAM	This study
pUDR472	colE1^{ori} 2-μm *bla aph* gRNA-TUP1 gRNA-TUP1	This study
pUDR473	colE1^{ori} 2-μm *bla aph* gRNA-ISW2 gRNA-ISW2	This study
pUDR566	colE1^{ori} 2-μm *bla aph* gRNA-BAS1 gRNA-BAS1	This study
pUDR592	colE1^{ori} 2-μm *bla aph* gRNA-hphNT1 gRNA-hphNT1	This study
pUDR652	colE1^{ori} 2-μm *bla aph* MX gRNA-FMS1 gRNA-FMS1	This study
pUDR651	colE1^{ori} 2-μm *bla aph* gRNA-SPE2 gRNA-SPE2	This study
pUDR514	colE1^{ori} 2-μm *bla aph* gRNA-YPRcTau3 gRNA-YPRcTau3	This study
pUDI180	colE1^{ori} *aph pTDH3-ScTHI4-tTDH1*	This study

two-step strategy was adopted where first the target gene to be mutated was removed and replaced with a synthetic and unique 20-bp target sequence plus 3-bp PAM sequence (SynPAM), and then the synthetic target sequence was targeted and replaced with the mutant gene. In the second step where the SynPAM sequence was targeted, the mutant gene flanked by about 400-bp upstream and downstream sequences was amplified by using the evolved strain genomic DNA as the template. The PCR product was then gel purified and used as a repair fragment in the transformation. This strategy yielded both intermediate strains lacking the targeted gene and final strains carrying the desired mutant gene.

In the first step, IMX585 was targeted at the gene of interest by transforming the strain with the relative pUDR plasmid. The double-strand break was then repaired by cotransforming the strain with two cDNA oligonucleotides carrying the SynPAM sequence flanked by 60-bp homology sequences to the targeted *locus* that were previously combined at a 1:1 molar ratio, boiled for 5 min, and annealed by cooling down the solution at room temperature on the bench.

Five hundred nanograms of annealed primer pairs 13612/13613, 13541/13542, 13539/13540, 14988/14989, 15075/15076, 13533/13534, 13531/13532, 13535/13536, and 13527/13528 were cotransformed with 500 ng pUDR388, pUDR389, pUDR390, pUDR438, pUDR412, pUDR441, pUDR472, pUDR473, and pUDR652, respectively, yielding IMX1721, IMX1722, IMX1723, IMX1988, IMX1820, IMX1819, IMX1817, IMX1818, and IMX2292, respectively. IMX1819 and IMX1820 transformants were selected on YPD plates with 200 mg/liter hygromycin, while IMX1721, IMX1722, IMX1723, IMX1988, IMX1817, IMX1818, and IMX2292 transformants were selected on YPD plates with 200 mg/liter G418.

The *BAS1* knockout strain could not be obtained with the marker-free SynPAM strategy. Therefore, the hphNT1 marker cassette was amplified by using primers 15584/15585 to add 60-bp homology flanks and pROS12 as a template. The PCR fragment was then gel purified, and 500 ng was cotransformed with 500 ng pUDR592 to yield IMX2128. Transformants were selected on YPD plates with 200 mg/liter G418 and 200 mg/liter hygromycin.

In the second step, the SynPAM target sequence in each knockout strain was targeted for the insertion of the mutant allele. The mutant gene flanked by approximately 400-bp upstream and downstream sequences was amplified using the evolved strain genomic DNA as the template. The PCR product was then gel purified, and 500 ng was cotransformed with 500 ng of pUDR471. Primer pairs 13523/13524, 11292/11293, 13525/13526, 12052/12053, 11725/11726, 13498/13499, 13498/13499, 15077/15078, 15077/15078, 13496/13497, and 13527/13528 were used to amplify the mutant alleles of *CNB1*^{L82F}, *PMR1*^{S104Y}, *FRE2*^{T110S}, *ARO7*^{L205S}, *ABZ1*^{R593H}, *GAL11*^{I541N}, *GAL11*^{Q383stop}, *TUP1*^{V374A}, *TUP1*^{Q99stop}, *ISW2*^{S181stop}, and *FMS1*^{Q33K}, respectively, using IMS0747, IMS0748, IMS0748, IMS0728, IMS0727, IMS0734, IMS0734, IMS0734, IMS0735, IMS0733, and IMS0735 genomic DNA as the templates, respectively. Transformants were selected on YPD plates with 200 mg/liter G418, yielding IMX1985, IMX1986, IMX1987, IMX1989, IMX2057, IMX1991, IMX1992, IMX2002, IMX2003, IMX1990, and IMX2292, respectively. The *BAS1*^{Q152R}, *BAS1*^{D101N}, and *BAS1*^{S41P} mutant alleles were amplified from IMS736, IMS737, and IMS738 genomic DNA, respectively, using the primer pair 13687/13688. After gel purification, 500 ng of each PCR product was cotransformed in IMX2128, together with the hphNT1-targeting plasmid pUDR650, yielding IMX2135, IMX2136, and IMX2137, respectively. The strain IMX2289 carrying the *SPE2*^{A278T} mutant allele was constructed by transforming IMX585 with the *SPE2*-targeting plasmid pUDR651 together with the annealed primer pair 16602/16603 containing the desired single base change plus a synonymous mutation causing the removal of the PAM sequence. After transformation, strains IMX2135, IMX2136, IMX2137, and IMX2289 were plated on YPD plates with 200 mg/liter G418 for selection.

Mutant alleles found in the same evolved strains were combined in a single strain by repeating the strategy described above but this time using a mutant strain as a starting point instead of IMX585. In this

way, *GAL11*, *TUP1*, and *FMS1* were deleted in IMX2002, IMX2003, and IMX2127, respectively, by cotransforming the relative gRNA plasmid and the relative double-stranded DNA (dsDNA) oligonucleotide pair as performed for the single-knockout strains, yielding the intermediate strains IMX2066, IMX2110, and IMX2294, respectively. Then, the SynPAM sequence was targeted in IMX2066, IMX2110, and IMX2294 as previously described for the single mutant strains, yielding IMX2087, IMX2127, and IMX2307, respectively. IMX2043 carrying the *PMR1*^S104Y^-*FRE2*^T110S^ double mutation was constructed by cotransforming IMX1987 with pUDR390 and the linear fragment containing the *FRE2*^T110S^ mutant allele that was previously amplified as described above. The *SPE2*^A278T^ mutant allele was combined with the *GAL11*^I541N^ *TUP1*^V374A^ mutant alleles present in IMX2127 by cotransforming the strain with the *SPE2*-targeting plasmid pUDR651 together with the annealed primer pair 16602/16603, yielding IMX2308. The *THI4* overexpression cassette was amplified by using pUDI180 as a template and primers 12174/12175. Five hundred nanograms of gel-purified PCR product was cotransformed together with the YPRcTau3-targeting plasmid pUDR514 in IMX585 and IMX1985 yielding IMX2290 and IMX2291, respectively.

To verify the correct gene editing, single colonies were picked from each transformation plate and genomic DNA was extracted as previously described (68). The targeted locus was amplified by PCR and run on a 1% agarose gel. Primers pair 13523/13524, 13541/13542, 13539/13540, 15077/15078, 13496/13497, 13498/13499, 12052/12053, 13523/13524, 13541/13542, 13539/13540, 13693/13694, 12052/12053, 13496/13497, 13498/13499, 13498/13499, 15077/15078, 15077/15078, 13524/13525, 13693/13694, 13498/13499, 15077/15078, 15077/15078, 13687/13688, 13498/13499, 13687/13688, 13687/13688, 13687/13688, 13261/13262, 13261/13262, 13492/13493, 13525/13526, 13525/13526, 13492/13493, and 13525/13526 were used to verify the correct gene editing in IMX1721, IMX1722, IMX1723, IMX1817, IMX1818, IMX1819, IMX1920, IMX1985, IMX1986, IMX1987, IMX1988, IMX1989, IMX1990, IMX1991, IMX1992, IMX2002, IMX2003, IMX2043, IMX2057, IMX2066, IMX2110, IMX2127, IMX2128, IMX2087, IMX2135, IMX2136, IMX2137 IMX2290, IMX2291, IMX2289, IMX2292, IMX2306, IMX2308, and IMX2307, respectively. To verify the presence of the single point mutations, each PCR product was purified and Sanger sequenced (Baseclear, The Netherlands). Mutations in *BAS1* could not be verified by Sanger sequencing; therefore, whole-genome resequencing of IMX2135, IMX2136, and IMX2137 was performed as explained above for the evolved single-colony isolates.

After genotyping of the transformants, correct isolates were grown in 20 ml YPD in a 50-ml vented Greiner tube at 30°C overnight by inoculating a single colony. The next day, 1 μl was transferred to a new tube containing the same amount of medium and the sample was grown overnight. The day after, each liquid culture was restreaked to single colony by plating on YPD agar plates. Plates were incubated at 30°C overnight, and the next day, single colonies were patched on both YPD and YPD plus the relative antibiotic (either G418 or hygromycin) to assess which clones had lost the gRNA plasmid. One clone for each strain that had lost the plasmid was then grown in YPD, and 30% (vol/vol) glycerol was added prior to stocking samples at −80°C.

Data availability. The sequencing data of the evolved and of the *BAS1* deletion *Saccharomyces cerevisiae* strains were deposited at NCBI (https://www.ncbi.nlm.nih.gov/) under BioProject accession number PRJNA603441. All measurement data used to prepare the figures of the manuscript are available at the data.4TU.nl repository (https://doi.org/10.4121/uuid:53c9992f-d004-4d26-a3cd-789c524fe35c).

REFERENCES

1. Bruinenberg PM, van Dijken JP, Scheffers WA. 1983. An enzymic analysis of NADPH production and consumption in *Candida utilis*. J Gen Microbiol 129:965–971. https://doi.org/10.1099/00221287-129-4-965.

2. Verduyn C, Postma E, Scheffers WA, Van Dijken JP. 1992. Effect of benzoic acid on metabolic fluxes in yeasts: a continuous-culture study on the regulation of respiration and alcoholic fermentation. Yeast 8:501–517. https://doi.org/10.1002/yea.320080703.

3. Sherman F, Fink G, Hicks J. 1987. Methods in yeast genetics: a laboratory course manual. Cold Spring Harbor Laboratory Press, Cold Spring Harbor, NY.

4. Combs GF. 2007. The vitamins. Elsevier Science, Amsterdam, Netherlands.

5. Perli T, Wronska AK, Ortiz-Merino RA, Pronk JT, Daran JM. 2020. Vitamin requirements and biosynthesis in *Saccharomyces cerevisiae*. Yeast 37:283–304. https://doi.org/10.1002/yea.3461.

6. Burkholder PR. 1943. Vitamin deficiencies in yeasts. Am J Bot 30:206–211. https://doi.org/10.1002/j.1537-2197.1943.tb14749.x.

7. Rogosa M. 1944. Vitamin requirements of lactose-fermenting and certain other yeasts. J Bacteriol 47:159–170. https://doi.org/10.1128/JB.47.2.159-170.1944.

8. de Kock SH, Du Preez JC, Kilian SG. 2000. The effect of vitamins and amino acids on glucose uptake in aerobic chemostat cultures of three *Saccharomyces cerevisiae* strains. Syst Appl Microbiol 23:41–46. https://doi.org/10.1016/S0723-2020(00)80044-2.

9. Burkholder PR, McVeigh I, Moyer D. 1944. Studies on some growth factors of yeasts. J Bacteriol 48:385–391. https://doi.org/10.1128/JB.48.4.385-391.1944.

10. Bracher JM, de Hulster E, Koster CC, van den Broek M, Daran JG, van Maris AJA, Pronk JT. 2017. Laboratory evolution of a biotin-requiring Saccharomyces cerevisiae strain for full biotin prototrophy and identification of causal mutations. Appl Environ Microbiol 83:e00892-17. https://doi.org/10.1128/AEM.00892-17.

11. Mans R, Daran JG, Pronk JT. 2018. Under pressure: evolutionary engineering of yeast strains for improved performance in fuels and chemicals production. Curr Opin Biotechnol 50:47–56. https://doi.org/10.1016/j.copbio.2017.10.011.

12. Sandberg TE, Salazar MJ, Weng LL, Palsson BO, Feist AM. 2019. The emergence of adaptive laboratory evolution as an efficient tool for biological discovery and industrial biotechnology. Metab Eng 56:1–16. https://doi.org/10.1016/j.ymben.2019.08.004.

13. Jansen MLA, Bracher JM, Papapetridis I, Verhoeven MD, de Bruijn H, de Waal PP, van Maris AJA, Klaassen P, Pronk JT. 2017. Saccharomyces cerevisiae strains for second-generation ethanol production: from academic exploration to industrial implementation. FEMS Yeast Res 17:fox044. https://doi.org/10.1093/femsyr/fox044.

14. Lynd LR, Elamder RT, Wyman CE. 1996. Likely features and costs of mature biomass ethanol technology. Appl Biochem Biotechnol 57–58:741–761. https://doi.org/10.1007/BF02941755.

15. Skinner KA, Leathers TD. 2004. Bacterial contaminants of fuel ethanol production. J Ind Microbiol Biotechnol 31:401–408. https://doi.org/10.1007/s10295-004-0159-0.

16. Perli T, Moonen DPI, van den Broek M, Pronk JT, Daran J-M. 2020. Adaptive laboratory evolution and reverse engineering of single-vitamin prototrophies in Saccharomyces cerevisiae. BioRxiv https://doi.org/10.1101/2020.02.12.945287.

17. Entian K-D, Kötter P. 2007. 25 yeast genetic strain and plasmid collections. Method Microbiol 36:629–666. https://doi.org/10.1016/S0580-9517(06)36025-4.

18. van Dijken JP, Bauer J, Brambilla L, Duboc P, Francois JM, Gancedo C, Giuseppin ML, Heijnen JJ, Hoare M, Lange HC, Madden EA, Niederberger P, Nielsen J, Parrou JL, Petit T, Porro D, Reuss M, van Riel N, Rizzi M, Steensma HY, Verrips CT, Vindelov J, Pronk JT. 2000. An interlaboratory comparison of physiological and genetic properties of four Saccharomyces cerevisiae strains. Enzyme Microb Technol 26:706–714. https://doi.org/10.1016/S0141-0229(00)00162-9.

19. Hassing EJ, de Groot PA, Marquenie VR, Pronk JT, Daran JG. 2019. Connecting central carbon and aromatic amino acid metabolisms to improve de novo 2-phenylethanol production in Saccharomyces cerevisiae. Metab Eng 56:165–180. https://doi.org/10.1016/j.ymben.2019.09.011.

20. Papapetridis I, van Dijk M, van Maris AJA, Pronk JT. 2017. Metabolic engineering strategies for optimizing acetate reduction, ethanol yield and osmotolerance in Saccharomyces cerevisiae. Biotechnol Biofuels 10:107. https://doi.org/10.1186/s13068-017-0791-3.

21. Kuijpers NG, Solis-Escalante D, Luttik MA, Bisschops MM, Boonekamp FJ, van den Broek M, Pronk JT, Daran JM, Daran-Lapujade P. 2016. Pathway swapping: toward modular engineering of essential cellular processes. Proc Natl Acad Sci U S A 113:15060–15065. https://doi.org/10.1073/pnas.1606701113.

22. Solis-Escalante D, Kuijpers NG, Barrajon-Simancas N, van den Broek M, Pronk JT, Daran JM, Daran-Lapujade P. 2015. A minimal set of glycolytic genes reveals strong redundancies in Saccharomyces cerevisiae central metabolism. Eukaryot Cell 14:804–816. https://doi.org/10.1128/EC.00064-15.

23. Salazar AN, Gorter de Vries AR, van den Broek M, Wijsman M, de la Torre Cortés P, Brickwedde A, Brouwers N, Daran J-M, Abeel T. 2017. Nanopore sequencing enables near-complete de novo assembly of Saccharomyces cerevisiae reference strain CEN.PK113-7D. FEMS Yeast Res 17:fox074. https://doi.org/10.1093/femsyr/fox074.

24. Chatterjee A, Abeydeera ND, Bale S, Pai P-J, Dorrestein PC, Russell DH, Ealick SE, Begley TP. 2011. Saccharomyces cerevisiae Thi4p is a suicide thiamine thiazole synthase. Nature 478:542–546. https://doi.org/10.1038/nature10503.

25. de Kok S, Nijkamp JF, Oud B, Roque FC, de Ridder D, Daran JM, Pronk JT, van Maris AJ. 2012. Laboratory evolution of new lactate transporter genes in a jen1Δ mutant of Saccharomyces cerevisiae and their identification as ADY2 alleles by whole-genome resequencing and transcriptome analysis. FEMS Yeast Res 12:359–374. https://doi.org/10.1111/j.1567-1364.2012.00787.x.

26. Ball SG, Wickner RB, Cottarel G, Schaus M, Tirtiaux C. 1986. Molecular

27. cloning and characterization of Aro7-Osm2, a single yeast gene necessary for chorismate mutase activity and growth in hypertonic medium. Mol Gen Genet 205:326–330. https://doi.org/10.1007/bf00430446.

27. Edman JC, Goldstein AL, Erbe JG. 1993. para-Aminobenzoate synthase gene of Saccharomyces cerevisiae encodes a bifunctional enzyme. Yeast 9:669–675. https://doi.org/10.1002/yea.320090613.

28. Rudolph HK, Antebi A, Fink GR, Buckley CM, Dorman TE, LeVitre J, Davidow LS, Mao JI, Moir DT. 1989. The yeast secretory pathway is perturbed by mutations in PMR1, a member of a Ca^{2+} ATPase family. Cell 58:133–145. https://doi.org/10.1016/0092-8674(89)90410-8.

29. Ton VK, Mandal D, Vahadji C, Rao R. 2002. Functional expression in yeast of the human secretory pathway Ca^{2+}, Mn^{2+}-ATPase defective in Hailey-Hailey disease. J Biol Chem 277:6422–6427. https://doi.org/10.1074/jbc.M110612200.

30. Cyert MS. 2003. Calcineurin signaling in Saccharomyces cerevisiae: how yeast go crazy in response to stress. Biochem Biophys Res Commun 311:1143–1150. https://doi.org/10.1016/S0006-291X(03)01552-3.

31. Lesuisse E, Blaiseau PL, Dancis A, Camadro JM. 2001. Siderophore uptake and use by the yeast Saccharomyces cerevisiae. Microbiology 147:289–298. https://doi.org/10.1099/00221287-147-2-289.

32. Yun CW, Tiedeman JS, Moore RE, Philpott CC. 2000. Siderophore-iron uptake in Saccharomyces cerevisiae. Identification of ferrichrome and fusarinine transporters. J Biol Chem 275:16354–16359. https://doi.org/10.1074/jbc.M001456200.

33. Tice-Baldwin K, Fink GR, Arndt KT. 1989. BAS1 has a Myb motif and activates HIS4 transcription only in combination with BAS2. Science 246:931–935. https://doi.org/10.1126/science.2683089.

34. Daignan-Fornier B, Fink GR. 1992. Coregulation of purine and histidine biosynthesis by the transcriptional activators BAS1 and BAS2. Proc Natl Acad Sci U S A 89:6746–6750. https://doi.org/10.1073/pnas.89.15.6746.

35. Zhang L, Guarente L. 1994. Evidence that TUP1/SSN6 has a positive effect on the activity of the yeast activator HAP1. Genetics 136:813–817.

36. Han SJ, Lee JS, Kang JS, Kim YJ. 2001. Med9/Cse2 and Gal11 modules are required for transcriptional repression of distinct group of genes. J Biol Chem 276:37020–37026. https://doi.org/10.1074/jbc.M105596200.

37. Fazzio TG, Gelbart ME, Tsukiyama T. 2005. Two distinct mechanisms of chromatin interaction by the Isw2 chromatin remodeling complex in vivo. Mol Cell Biol 25:9165–9174. https://doi.org/10.1128/MCB.25.21.9165-9174.2005.

38. Whitney PA, Morris DR. 1978. Polyamine auxotrophs of Saccharomyces cerevisiae. J Bacteriol 134:214–220. https://doi.org/10.1128/JB.134.1.214-220.1978.

39. Joets J, Pousset D, Marcireau C, Karst F. 1996. Characterization of the Saccharomyces cerevisiae FMS1 gene related to Candida albicans corticosteroid-binding protein 1. Curr Genet 30:115–120. https://doi.org/10.1007/s002940050109.

40. Flagfeldt DB, Siewers V, Huang L, Nielsen J. 2009. Characterization of chromosomal integration sites for heterologous gene expression in Saccharomyces cerevisiae. Yeast 26:545–551. https://doi.org/10.1002/yea.1705.

41. Panozzo C, Nawara M, Suski C, Kucharczyka R, Skoneczny M, Becam AM, Rytka J, Herbert CJ. 2002. Aerobic and anaerobic NAD^+ metabolism in Saccharomyces cerevisiae. FEBS Lett 517:97–102. https://doi.org/10.1016/S0014-5793(02)02585-1.

42. Subramanian M, Qiao WB, Khanam N, Wilkins O, Der SD, Lalich JD, Bognar AL. 2005. Transcriptional regulation of the one-carbon metabolism regulon in Saccharomyces cerevisiae by Bas1p. Mol Microbiol 57:53–69. https://doi.org/10.1111/j.1365-2958.2005.04663.x.

43. Dong YX, Sueda S, Nikawa J, Kondo H. 2004. Characterization of the products of the genes SNO1 and SNZ1 involved in pyridoxine synthesis in Saccharomyces cerevisiae. Eur J Biochem 271:745–752. https://doi.org/10.1111/j.1432-1033.2003.03973.x.

44. Teixeira MC, Monteiro PT, Palma M, Costa C, Godinho CP, Pais P, Cavalheiro M, Antunes M, Lemos A, Pedreira T, Sa-Correia I. 2018. YEASTRACT: an upgraded database for the analysis of transcription regulatory networks in Saccharomyces cerevisiae. Nucleic Acids Res 46:D348–D353. https://doi.org/10.1093/nar/gkx842.

45. Mieczkowski PA, Dominska M, Buck MJ, Gerton JL, Lieb JD, Petes TD. 2006. Global analysis of the relationship between the binding of the Bas1p transcription factor and meiosis-specific double-strand DNA breaks in Saccharomyces cerevisiae. Mol Cell Biol 26:1014–1027. https://doi.org/10.1128/MCB.26.3.1014-1027.2006.

46. Fendt SM, Oliveira AP, Christen S, Picotti P, Dechant RC, Sauer U. 2010. Unraveling condition-dependent networks of transcription factors that

control metabolic pathway activity in yeast. Mol Syst Biol 6:432. https://doi.org/10.1038/msb.2010.91.

47. Papamichos-Chronakis M, Conlan RS, Gounalaki N, Copf T, Tzamarias D. 2000. Hrs1/Med3 is a Cyc8-Tup1 corepressor target in the RNA polymerase II holoenzyme. J Biol Chem 275:8397–8403. https://doi.org/10.1074/jbc.275.12.8397.

48. Komachi K, Johnson AD. 1997. Residues in the WD repeats of Tup1 required for interaction with alpha2. Mol Cell Biol 17:6023–6028. https://doi.org/10.1128/mcb.17.10.6023.

49. Proft M, Pascual-Ahuir A, de Nadal E, Ariño J, Serrano R, Posas F. 2001. Regulation of the Sko1 transcriptional repressor by the Hog1 MAP kinase in response to osmotic stress. EMBO J 20:1123–1133. https://doi.org/10.1093/emboj/20.5.1123.

50. Cooper JP, Roth SY, Simpson RT. 1994. The global transcriptional regulators, *SSN6* and *TUP1*, play distinct roles in the establishment of a repressive chromatin structure. Genes Dev 8:1400–1410. https://doi.org/10.1101/gad.8.12.1400.

51. Mizuno T, Harashima S. 2003. Gal11 is a general activator of basal transcription, whose activity is regulated by the general repressor Sin4 in yeast. Mol Genet Genomics 269:68–77. https://doi.org/10.1007/s00438-003-0810-x.

52. Giaever G, Chu AM, Ni L, Connelly C, Riles L, Véronneau S, Dow S, Lucau-Danila A, Anderson K, André B, Arkin AP, Astromoff A, El-Bakkoury M, Bangham R, Benito R, Brachat S, Campanaro S, Curtiss M, Davis K, Deutschbauer A, Entian K-D, Flaherty P, Foury F, Garfinkel DJ, Gerstein M, Gotte D, Güldener U, Hegemann JH, Hempel S, Herman Z, Jaramillo DF, Kelly DE, Kelly SL, Kötter P, LaBonte D, Lamb DC, Lan N, Liang H, Liao H, Liu L, Luo C, Lussier M, Mao R, Menard P, Ooi SL, Revuelta JL, Roberts CJ, Rose M, Ross-Macdonald P, Scherens B, et al. 2002. Functional profiling of the *Saccharomyces cerevisiae* genome. Nature 418:387–391. https://doi.org/10.1038/nature00935.

53. Jedidi I, Zhang F, Qiu H, Stahl SJ, Palmer I, Kaufman JD, Nadaud PS, Mukherjee S, Wingfield PT, Jaroniec CP, Hinnebusch AG. 2010. Activator Gcn4 employs multiple segments of Med15/Gal11, including the KIX domain, to recruit mediator to target genes *in vivo*. J Biol Chem 285:2438–2455. https://doi.org/10.1074/jbc.M109.071589.

54. Tsukiyama T, Palmer J, Landel CC, Shiloach J, Wu C. 1999. Characterization of the imitation switch subfamily of ATP-dependent chromatin-remodeling factors in *Saccharomyces cerevisiae*. Genes Dev 13:686–697. https://doi.org/10.1101/gad.13.6.686.

55. Georgatsou E, Alexandraki D. 1994. Two distinctly regulated genes are required for ferric reduction, the first step of iron uptake in *Saccharomyces cerevisiae*. Mol Cell Biol 14:3065–3073. https://doi.org/10.1128/mcb.14.5.3065.

56. Antebi A, Fink GR. 1992. The yeast Ca²⁺-ATPase homolog, Pmr1, is required for normal Golgi function and localizes in a novel Golgi-like distribution. Mol Biol Cell 3:633–654. https://doi.org/10.1091/mbc.3.6.633.

57. Nosaka K, Nishimura H, Kawasaki Y, Tsujihara T, Iwashima A. 1994. Isolation and characterization of the *THI6* gene encoding a bifunctional thiamin-phosphate pyrophosphorylase/hydroxyethylthiazole kinase from *Saccharomyces cerevisiae*. J Biol Chem 269:30510–30516.

58. Llorente B, Fairhead C, Dujon B. 1999. Genetic redundancy and gene fusion in the genome of the Baker's yeast *Saccharomyces cerevisiae*: functional characterization of a three-member gene family involved in the thiamine biosynthetic pathway. Mol Microbiol 32:1140–1152. https://doi.org/10.1046/j.1365-2958.1999.01412.x.

59. Steynparve EP. 1952. Partial purification and properties of thiaminokinase from yeast. Biochim Biophys Acta 8:310–324. https://doi.org/10.1016/0006-3002(52)90046-2.

60. Verhoeven MD, Lee M, Kamoen L, van den Broek M, Janssen DB, Daran

J-M, van Maris AJA, Pronk JT. 2017. Mutations in *PMR1* stimulate xylose isomerase activity and anaerobic growth on xylose of engineered *Saccharomyces cerevisiae* by influencing manganese homeostasis. Sci Rep 7:46155–46155. https://doi.org/10.1038/srep46155.

61. Alper H, Moxley J, Nevoigt E, Fink GR, Stephanopoulos G. 2006. Engineering yeast transcription machinery for improved ethanol tolerance and production. Science 314:1565–1568. https://doi.org/10.1126/science.1131969.

62. Chatterjee A, Jurgenson CT, Schroeder FC, Ealick SE, Begley TP. 2007. Biosynthesis of thiamin thiazole in eukaryotes: conversion of NAD to an advanced intermediate. J Am Chem Soc 129:2914–2922. https://doi.org/10.1021/ja067606t.

63. Chatterjee A, Schroeder FC, Jurgenson CT, Ealick SE, Begley TP. 2008. Biosynthesis of the thiamin-thiazole in eukaryotes: identification of a thiazole tautomer intermediate. J Am Chem Soc 130:11394–11398. https://doi.org/10.1021/ja802140a.

64. Bachmann H, Bruggeman FJ, Molenaar D, Branco Dos Santos F, Teusink B. 2016. Public goods and metabolic strategies. Curr Opin Microbiol 31:109–115. https://doi.org/10.1016/j.mib.2016.03.007.

65. Nilsson A, Nielsen J. 2016. Metabolic trade-offs in yeast are caused by F₁F₀-ATP synthase. Sci Rep 6:22264. https://doi.org/10.1038/srep22264.

66. Wronska AK, Haak MP, Geraats E, Bruins Slot E, van den Broek M, Pronk JT, Daran JG. 10 April 2020. Exploiting the diversity of *Saccharomycotina* yeasts to engineer biotin-independent growth of *Saccharomyces cerevisiae*. Appl Environ Microbiol https://doi.org/10.1128/AEM.00270-20.

67. Nijkamp JF, van den Broek M, Datema E, de Kok S, Bosman L, Luttik MA, Daran-Lapujade P, Vongsangnak W, Nielsen J, Heijne WH, Klaassen P, Paddon CJ, Platt D, Kotter P, van Ham RC, Reinders MJ, Pronk JT, de Ridder D, Daran JM. 2012. *De novo* sequencing, assembly and analysis of the genome of the laboratory strain *Saccharomyces cerevisiae* CEN.PK113-7D, a model for modern industrial biotechnology. Microb Cell Fact 11:36. https://doi.org/10.1186/1475-2859-11-36.

68. Looke M, Kristjuhan K, Kristjuhan A. 2011. Extraction of genomic DNA from yeasts for PCR-based applications. Biotechniques 50:325–328. https://doi.org/10.2144/000113672.

69. Gietz RD, Woods RA. 2002. Transformation of yeast by lithium acetate/single-stranded carrier DNA/polyethylene glycol method. Methods Enzymol 350:87–96. https://doi.org/10.1016/s0076-6879(02)50957-5.

70. Inoue H, Nojima H, Okayama H. 1990. High efficiency transformation of *Escherichia coli* with plasmids. Gene 96:23–28. https://doi.org/10.1016/0378-1119(90)90336-p.

71. Nijkamp JF, van den Broek MA, Geertman JM, Reinders MJ, Daran JM, de Ridder D. 2012. *De novo* detection of copy number variation by co-assembly. Bioinformatics 28:3195–3202. https://doi.org/10.1093/bioinformatics/bts601.

72. Mans R, Wijsman M, Daran-Lapujade P, Daran JM. 2018. A protocol for introduction of multiple genetic modifications in *Saccharomyces cerevisiae* using CRISPR/Cas9. FEMS Yeast Res 18:foy063. https://doi.org/10.1093/femsyr/foy063.

73. Mans R, van Rossum HM, Wijsman M, Backx A, Kuijpers NG, van den Broek M, Daran-Lapujade P, Pronk JT, van Maris AJ, Daran JM. 2015. CRISPR/Cas9: a molecular Swiss army knife for simultaneous introduction of multiple genetic modifications in *Saccharomyces cerevisiae*. FEMS Yeast Res 15:fov004. https://doi.org/10.1093/femsyr/fov004.

74. Lee ME, DeLoache WC, Cervantes B, Dueber JE. 2015. A highly characterized yeast toolkit for modular, multipart assembly. ACS Synth Biol 4:975–986. https://doi.org/10.1021/sb500366v.

75. Fordyce PM, Gerber D, Tran D, Zheng J, Li H, DeRisi JL, Quake SR. 2010. *De novo* identification and biophysical characterization of transcription-factor binding sites with microfluidic affinity analysis. Nat Biotechnol 28:970–975. https://doi.org/10.1038/nbt.1675.